for BCL2 protein was classified as positive if more than 50% of lymphoma cells were stained.[29]

We also classified *de novo* CD5⁺ DLBCL into two subgroups, i.e., germinal center B-cell and non-germinal center B-cell types.[30] From the file of histological consultation for diagnosis at the Aichi Cancer Center in the period from 2000 to 2004, 44 cases of *de novo* CD5⁺ DLBCL were selected for this analysis. Staining for CD10, BCL6 (NCL-BCL6, Novocastra), and MUM1 (MUM1p, DAKO) was performed on paraffin sections.[30] Cases were considered positive if 30% or more of the neoplastic cells were stained with an antibody. Subsequently, each case was classified into germinal center or non-germinal center B-cell types according to the criteria of Hans *et al.*[30]

Statistical analysis

Correlations between the two groups were examined with the χ^2 test and Fisher's exact test. Patients' survival data were analyzed with the Kaplan-Meier method and were compared by means of the log-rank test. Univariate and multivariate analyses were performed with the Cox proportional hazard regression model, and data were analyzed with STATA software (version 9.0, STATA Corp., College Station, TX, USA).

Results

Histopathological review and characterization of morphological variants

At a low magnification, total or partial effacement of the nodal architecture with a diffuse 118 patients, 98% or vaguely nodular pattern 2 patients, 2% of tumor cell proliferation was observed. In ten patients 8%, these tumor cells were distributed throughout the interfollicular area, while the follicles which had retained their mantle cuffs were spared.

In the current study, particular attention was paid to the presence or absence of intravascular and/or sinusoidal patterns. Although the extent of such patterns varied in each case, they were seen in 45 cases examined 38%. In the specimens of lymph node obtained from 31 patients, tumor cells infiltrated diffusely and focal intrasinusoidal infiltration was observed simultaneously. In the specimens of bone marrow from seven patients, spleen from two patients, and Waldeyer's ring from one patient, lymphoma cells were observed mainly in the sinusoids. In the other patients, a specimen was taken from the tumor in the nasal cavity, stomach, breast, and testis. In those specimens, lymphoma cells infiltrated diffusely, and focal intravascular infiltration was also observed. There was no significant difference in the incidence of intravascular and/or sinusoidal patterns between lymphatic 34/85, 40% and extranodal 11/35, 31% specimens.

The size of tumor cells was medium-to-large in 19 cases, mixed medium and large in 14 cases, and large in 87 cases. The tumor cells generally showed a scant or moderate rim of pale baso- or amphophilic cytoplasm. Of note, bi-nucleated tumor cells with a *snowman-like* morphology were frequently observed in our series (101 out of 120 cases, 85%) (Figures 1A and 2B). Apoptotic cells were observed in 21% of the cases.

We classified *de novo* CD5⁺ DLBCL according to cytomorphological features Figure 1. In 91 76% of 120 patients, monomorphic proliferation of typical centroblasts was observed, although a few scattered giant cells were seen in nine patients. We regarded these features as the prototype of *de novo* CD5⁺ DLBCL and referred to it as the common variant. In 13 11% out of the remaining patients, there was an increase in very large cells with giant or multiple nuclei, varying from 10 to 30% in area and intermixed with centroblasts and immunoblasts. We referred to this as the giant cell-rich variant. This could correspond to the anaplastic variant of DLBCL according to the WHO classification.[2] While the giant cell-rich variant was thus shown to have a polymorphous composition, monomorphous areas with relatively small cells were also usually identified, suggesting that there is a histological continuum between the common and giant cell-rich variants. CD30 was positive in 23% of the cases 3/13. In 14 patients 12%, tumor cells showed irregularly shaped nuclei,

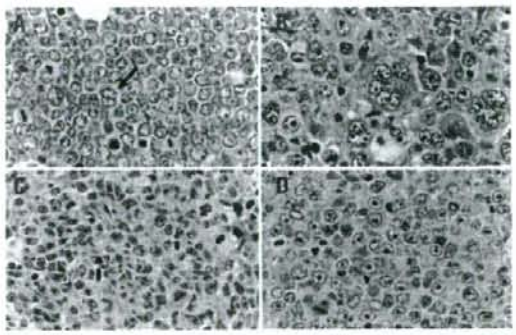

Figure 1. Cytomorphologic features of four variants of *de novo* CD5⁺ DLBCL. The cells, varying from medium to large in size, are uniform, with a pale basophilic or amphophilic cytoplasm. (A) Common variant, which can be described as the monomorphic or centroblastic variant. *Snowman-like*, bi-nucleated cells were seen (arrow). (B) Giant cell-rich variant. (C) Polymorphic variant, characterized by polymorphous proliferation with medium and large-sized cells. The immunoblastic variant (D) was rare in our case series.

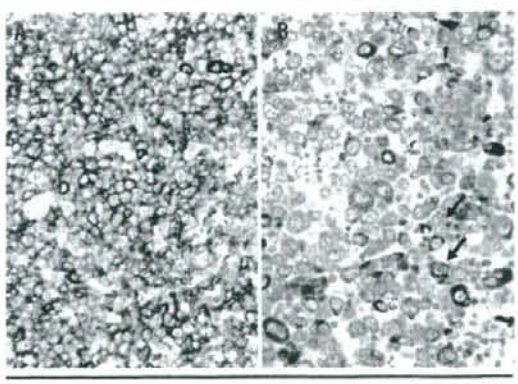

Figure 2. Immunohistochemical features of *de novo* CD5⁺ DLBCL. Lymphoma cells are positive for CD5 (A) and BCL2 (B). *Snowman-like*, bi-nucleated cells can be seen (arrow).

i.e., indented or multilobated, and were usually characterized by a mixed morphology, which was referred to as the polymorphic variant. Pure proliferation of immunoblasts was seen in only two patients 1%, and was termed the immunoblastic variant. Intravascular/sinusoidal infiltration was observed in 26% of the common variants, 62% of the giant cell-rich variants, 14% of the polymorphic variants, and 0% of the immunoblastic variants. The giant cell-rich variant was associated with intravascular/sinusoidal infiltration more frequently than the common variant (p=0.01).

Clinical features according to morphological variants

The patients' main characteristics and therapeutic results according to morphological categorization are summarized in Table 1. We compared the clinical characteristics between the current group of 120 patients with *de novo* CD5$^+$ DLBCL and 384 patients with CD5$^-$ DLBCL in our previous study.[11] Our previous findings on the clinical features of *de novo* CD5$^+$ DLBCL such as an older age, at onset, female predominance, frequent extranodal involvement, and higher International Prognostic Index IPI [31] score were confirmed in the current group of 120 patients (*data not shown*).

Table 1. Clinical features of the patients with *de novo* CD5$^+$ diffuse large B-cell lymphoma.

	Total *n=120* %	*Common* *n=91* %	*Giant cell-rich* *n=13* %	*Polymorphic* *n=14* %	*Immunoblastic* *n=2* %
Age at diagnosis, years.					
Median	66	66	63	67/71	62/69
Range	22-91	22-91	36-81	52-89	62,69
Over 60 years old	84 70	64 70	9 69	9 64	2 100
Sex male:female	58:62	40:51	9:4	8:6	1:1
Performance status >1	39 33	27 30	4 31	6 43	2 100
Serum LDH level >normal	85 71	61 67	11 85	11 79	2 100
Stage III/IV	73 61	54 59	9 69	8 57	2 100
Extranodal involvement	75 63	55 60	8 62	11 79	1 50
More than one site	29 24	20 22	4 31	5 36	0 0
International Prognostic Index					
Low	30 25	25 27	1 8	4 29	0 0
Low-intermediate	30 25	26 29	4 31	0 0	0 0
High-intermediate	19 16	11 12	4 31	4 29	0 0
High	41 34	29 32	4 31	6 43	2 100
B-symptoms present	49/117 44	35/88 40	5 38	7 50	2 100
Complete response rate	77/114 68	64/86 74	5/12 42	7/14 50	1/2 50
5-year OS rate	38	44	15	21	0

LDH: lactate dehydrogenase; OS: overall survival.

The clinical features, including the five factors of the IPI,[31] were not significantly different among the four morphological variants of *de novo* CD5$^+$ DLBCL. The bone marrow, liver, and spleen were the most frequently involved anatomical sites irrespective of the morphological variant (*data not shown*).

Atypical lymphocyte concentrations (range, 11 to 78%) were noted at presentation in the peripheral blood smear of four cases, whose white blood cell counts ranged from 6,000 to 41,000/mm^3. None of these patients showed marked splenomegaly and the morphology of leukemic cells differed from that of B-cell prolymphocytic leukemia cells.

Immunophenotypic features

BCL2 protein was expressed in 86 out of 96 tumors, and observed in more than 70% of the tumor cells in almost all positive cases Figure 2B. This incidence was significantly higher than that in the CD5$^-$ DLBCL cases (105/150, 70%; p=0.0003).

As for the molecular classification system established by Hans *et al.*,[30] 36 of 44 cases 82% of *de novo* CD5$^+$ DLBCL were classified as the non-germinal center B-cell type. Thirty patients 68% showed the CD10$^-$BCL6$^-$MUM1$^+$ immunophenotype. CD10 was positive in seven patients 16%, BCL6 was negative in 79% of the cases examined 33/42, and MUM1 was positive in 95% of the cases 42/44. Only one patient showed the CD10$^+$BCL6$^+$MUM1$^-$ immunophenotype.

Among the four morphological variants, the common variant was positive for Ig-κ more frequently than either the giant cell-rich (p=0.05) or polymorphic (p=0.03) variant. As for other expression of other antigens there were no significant differences among the morphological variants of *de novo* CD5$^+$ DLBCL (*data not shown*).

Therapeutic outcome and long-term survival according to histopathological variants

Clinical follow-up data and information about the first-line therapy were available for all patients. The treatment consisted of chemotherapeutic regimens including anthracycline for 104 patients and without anthracycline for three. No patient was treated with rituximab in the first-line therapy. Seven patients with localized disease were treated with radiotherapy or surgical resection alone as first-line therapy. Six patients who did not receive any therapy because of their poor performance status all died of their disease. A complete response was achieved on first-line therapy in 77 68% out of the 114 patients who received treatment. Seven patients were lost to follow-up within 5 years after the diagnosis. The median observation time of surviving patients was 81 months. The 2-year overall survival rate of all 120 patients, estimated by the Kaplan-Meier method, was 52%, and the 5-year overall survival rate was 38% (Figure 3A).

We collected data on sites of involvement at relapse/progression. Among all 120 patients with *de novo* CD5$^+$ DLBCL, 16 patients 13% developed central nervous system (CNS) recurrence (Table 2). All these patients were treated with anthracycline-containing chemotherapy as a front-line treatment. One patient had brain

involvement at diagnosis. She achieved a complete response following front-line therapy, but develop recurrence in the thoracic spinal cord. The other patients did not show any CNS involvement at diagnosis. Twelve patients experienced CNS relapse after achieving a complete response. Of these, eight experienced isolated CNS relapse while the CNS relapse was associated with a systemic relapse in the others. Four patients experienced CNS disease progression during the first-line treatment. The median age of all 16 patients with CNS relapse was 64 years range, 28 to 85. Of note, all but three patients were over 60 years old. Seven were male and nine were female. The serum lactate dehydrogenase level was elevated in 13 of these patients and performance status was higher than one in seven patients. Five patients showed more than one extranodal site of involvement. Nine patients were categorized as having a high-intermediate or high risk, according to the IPI. The median time from diagnosis to CNS recurrence was 16 months. We compared therapeutic outcome and survival data in the 120 paients with *de novo* CD5⁺ DLBCL according to the morphological variants. The complete response rate was lowest 42% in patients with the giant cell-rich variant of *de novo* CD5⁺ DLBCL, and was significant different from that in patients with the common variant (p=0.02, Table 1). Five-year overall survival rates for patients with common, giant cell-rich, polymorphic, and immunoblastic variants were 44%, 15%, 21%, and 0%, respectively (Table 1, Figure 3B). The survival curve of patients with the common variant was significantly better than that of patients with the other three variants combined (p=0.011, Figure 3C). The presence of intravascular/sinu-

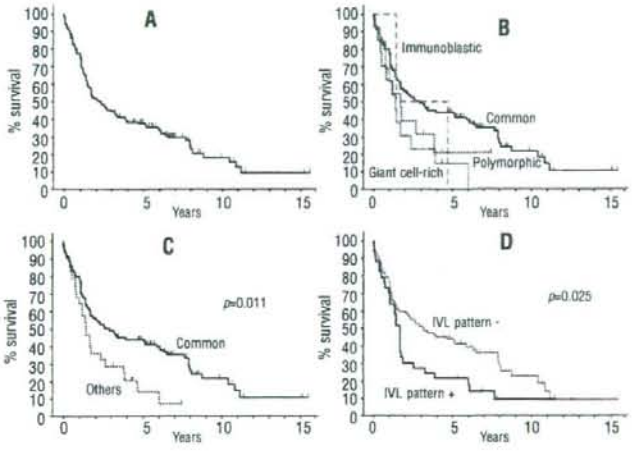

Figure 3. Survival according to the histological features of *de novo* CD5⁺ diffuse large B-cell lymphoma (DLBCL). (A) Overall survival in all 120 patients with *de novo* CD5⁺ DLBCL. (B) Overall survival of patients with different histological variants of *de novo* CD5⁺ DLBCL. (C) Patients with the common variant had a better survival than those with the other three variants of *de novo* CD5⁺ DLBCL. (D) The presence of intravascular/sinusoidal infiltration had an impact on the overall survival. IVL, intravascular/sinusoidal.

Table 2. Clinicopathological features of patients with *de novo* CD5⁺ diffuse large B-cell lymphoma who experienced central nervous system recurrence.

N.	*Age/sex*	*Stage*	*Sites of extranodal involvement*	*PS >1*	*LDH >N*	*IPI score*	*Histological variant*	*IVL pattern*	*CR*	*Sites of recurrence*	*Period from diagnosis to CNS recurrence months*	*Survival, months outcome*
1	62/M	IIIA	Lung, stomach, kidney, gingiva		Y	4	Common			CNS	2	8, DOD
2	77/M	IA		Y	Y	3	Polymorphic			CNS	2	4, DOD
3	76/M	IIA			Y	2	Common			CNS	3	9, DOD
4	61/F	IVB	BM	Y	Y	4	Common	Y	Y	CNS	5	9, DOD
5	67/M	IVB	Liver, BM	Y	Y	5	Common	Y	Y	CNS	6	23, DOD
6	85/M	IIIA		Y	Y	4	Common			CNS	<7	7, DOD
7	62/F	IIIA	Brain, pleura	Y	Y	5	Common	Y	Y	CNS	8	18, DOD
8	62/F	IIIB		Y	Y	4	Immunoblastic		Y	CNS, LN, liver, ascites, BM	8	18, DOD
9	38/F	IVB	BM		Y	2	Common		Y	CNS	24	72, DOD
10	66/F	III	Bone, uterus		Y	4	Common		Y	CNS intraocular	37	43, AWD
11	62/M	IVB	Liver, BM	Y	Y	5	Common		Y	Pelvis,CNS	39	40, DOD
12	28/F	IIA	Breast			0	Common		Y	CNS intraocular	57	86, AWD
13	50/M	IIIB			Y	2	Giant cell-rich	Y	Y	CNS	60	74, DOD
14	69/F	IA				1	Common		Y	CNS, etc.	71	80, DOD
15	67/F	IA			Y	2	Common	Y	Y	CNS intraocular	84	84, AWD
16	74/F	IA				1	Common		Y	CNS, LN	96	99, DOD

PS: performance status; LDH: lactate dehydrogenase; IVL: intravascular/sinusoidal; CR: complete response; Y: yes; BM: bone marrow; LN: lymph node; DOD: died of disease; AWD: alive with disease.

soidal infiltration also had an impact on survival (p=0.025, Figure 3D). The results of univariate and multivariate analyses to assess the impact of clinical and morphologic features on overall survival in *de novo* CD5$^+$ DLBCL patients are shown in Table 3. Univariate analysis identified the five risk factors of IPI, morphological variants, and intravascular/sinusoidal infiltration as prognostic factors important for overall survival. The presence of either *snowman-like* cells or a higher mitotic ratio > 4/one high-power field on average was not associated with a reduced overall survival (*data not shown*). Multivariate analysis adjusted for the five risk factors of the IPI confirmed the independent prognostic significance of histological categorization for overall survival (Table 3). Among the prognostic factors, the morphologic variant, age, performance status, and serum lactate dehydrogenase level were significantly associated with survival.

Table 3. **Prognostic factors affecting overall survival of patients with *de novo* CD5$^+$ diffuse large B-cell lymphoma.**

		Univariate			Multivariate		
Variables	*Unfavorable factor*	*HR*	*CI*	*p*	*HR*	*CI*	*p*
Comparison with risk factors							
Morphological variants	Not common	1.85	1.14-3.01	0.01	1.67	1.02-2.75	0.04
IVL pattern	Present	1.66	1.06-2.60	0.03		-	-
Age	>60 years	2.37	1.44-3.92	0.001	1.91	1.15-3.19	0.01
Performance status	2-4	2.81	1.81-4.37	<0.001	1.77	1.11-2.85	0.02
LDH	>Normal	3.71	2.14-6.43	<0.001	2.56	(1.43-4.61)	0.002
Stage	III/IV	2.34	1.48-3.69	<0.001		-	-
Extranodal diseases	>1 site	1.72	1.07-2.77	0.03		-	-
B symptoms	Present	2.09	1.36-3.19	<0.001		-	-
Comparison with IPI category							
Morphological variants	Not common	1.85	1.14-3.01	0.01	1.44	0.87-2.36	0.15
IPI category	HI/H	3.32	2.14-5.15	<0.001	3.14	2.00-4.92	<0.001
IVL pattern	Present	1.66	1.06-2.60	0.03	1.81	1.14-2.86	0.01
IPI category	HI/H	3.32	2.14-5.15	<0.001	3.46	2.21-5.41	<0.001

HR: hazard ratio; CI:confidence interval; HI/H: high-intermediate or high risk category of IPI; IVL: intravascular/sinusoidal; LDH, lactate dehydrogenase.

Discussion

We clarified detailed cytomorphological features of *de novo* CD5$^+$ DLBCL. A German study also documented morphological features in their series of 13 cases of *de novo* CD5$^+$ DLBCL, identifying eight centroblastic 62%, three immunoblastic 23%, and two unclassified DLBCL with irregular nuclei 15%. [13] Our findings generally appeared to be in keeping with those of the German study; however, the percentage of immunoblastic lymphoma cases 23% was higher in the German study than in ours 2%. DLBCL developing in the setting of small lymphocytic lymphoma/chronic lymphocytic leukemia (Richter's syndrome) evidently tend to be characterized by an immunoblastic morphology and the expression of CD5.[32] In Japan, the incidence of chronic lymphocytic leukemia is one fifth of that in Western countries.[33,34] Moreover, CD5 expression was mainly examined using fresh material in the majority of studies of *de novo* CD5$^+$ DLBCL in Japan, while it was examined in paraffin-embedded material in the studies in Western countries. In Japan, the incidence of *de novo* CD5$^+$ DLBCL ranges from 4% 4/101 [35] to 10% 24/240, [36] which seems to be almost the same as that reported in Western series.[10,37] Since only two cases have been included in the current study, the clinicopathological features of the immunoblastic variant of *de novo* CD5$^+$ DLBCL remain unknown. International cooperative studies are needed to verify the hypothesis that these facts may explain the conflicting data. Since *de novo* CD5$^+$ DLBCL has various histopathological appearances, CD5 immunostaining should be performed routinely in cases of DLBCL.

In the current study, intravascular/sinusoidal patterns to various extents were observed in 38% of the cases of *de novo* CD5$^+$ DLBCL. As Murase *et al.* demonstrated recently,[21] *de novo* CD5$^+$ DLBCL with an intravascular/sinusoidal pattern showed intermediate features in terms of aggressive clinical behavior and prognosis between *de novo* CD5$^+$ DLBCL without an intravascular/sinusoidal pattern and CD5$^+$ intravascular large B-cell lymphoma, suggesting that a part of the two diseases overlaps. In the present study *snowman-like*, binucleated cells were frequently observed in *de novo* CD5$^+$ DLBCL. Further studies in CD5$^-$ DLBCL and CD5$^+$ intravascular large B-cell lymphoma are needed to evaluate their diagnostic significance in *de novo* CD5$^+$ DLBCL.

The aggressive clinical feature of *de novo* CD5$^+$ DLBCL that we previously reported[11] was confirmed by the current study and a recent study that was conducted using tumor specimens from patients with DLBCL uniformly treated with anthracycline-based chemotherapeutic regimens in a prospective, multi-center clinical trial.[37] In contrast, it has been reported that the expression of CD5 in DLBCL did not affect overall survival.[13] Recent studies revealed that patients with *de novo* CD5$^+$ DLBCL with 8p21-associated chromosomal abnormalities[15] and with 9p21 loss in comparative genomic hybridization analysis[16] have an extremely short survival. The existence of these highly aggressive subgroups of *de novo* CD5$^+$ DLBCL may explain the heterogeneity in the prognosis of this disease. The possible role of the CD5 molecule in the aggressiveness of *de novo* CD5$^+$ DLBCL remains unknown. It has been reported that CD5 supports the survival of B cells by stimulating the production of interleukin-10 and by down-regulating B-cell receptor signaling.[38] This molecular basis may explain in part why *de novo* CD5$^+$ DLBCL shows more aggressive clinical features than CD5$^-$ DLBCL.

According to the criteria established by Hans *et al.*,[30] 82% of the cases examined in the present study were non-germinal center B-cell DLBCL. Our results suggest that *de novo* CD5$^+$ DLBCL is mainly classified into the non-germinal center B-cell type, and may provide a clue to clarify the aggressiveness of such DLBCL. Our present study also revealed that *de novo* CD5$^+$ DLBCL typically shows the BCL2$^+$ BCL6$^-$ immunophenotype.

Recent clinical studies suggest that the prognosis of DLBCL expressing BCL2 protein, BCL6 protein-negative DLBCL, and DLBCL of the non-germinal center B-cell subgroup is improved by rituximab-containing chemotherapy.[39-41] In our previous study published in 2002, no patients had been treated with rituximab.[11] In the present study, some patients had been treated with rituximab as a part of salvage therapy; however, the overall survival was almost the same as that in the previous study and was not clearly improved. The therapeutic impact of adding rituximab to first-line therapy in *de novo* CD5+ DLBCL needs to be evaluated in the setting of a well-designed clinical trial.

The overall incidence of CNS recurrence in aggressive non-Hodgkin's lymphoma excluding lymphoblastic lymphoma/acute lymphoblastic leukemia and Burkitt's lymphoma is approximately 5%,[42-44] and the incidence in DLBCL seems to be less than 5%. The incidence of CNS recurrence in the present study, 13%, was marked. Most of our patients with CNS recurrence had an elevated level of serum lactate dehydrogenase, which has been reported as a potential risk factor for CNS recurrence in aggressive lymphoma.[42] In contrast, most of the patients with CNS recurrence were over 60 years old, which was reported to be a favorable factor in a study of a large number of patients.[42] To establish an optimal therapeutic strategy for CNS prophylaxis in DLBCL, the relationship between CD5 expression and CNS recurrence in DLBCL should be examined in future studies.

In conclusion, our study provides new clinicopathological information on *de novo* CD5+ DLBCL. *De novo* CD5+ DLBCL shows many unique clinicopathological and genetic features. Further studies are needed to clarify molecular mechanisms in highly aggressive subgroups of *de novo* CD5+ DLBCL.

Appendix

List of participating institutes in the CD5+ DLBCL histology project: Akita University School of Medicine, Akita Kumiai General Hospital, National Miyagi Hospital, Saka General Hospital, Tohoku University School of Medicine, Sendai City Hospital, Furukawa City Hospital, Fukushima Medical College, Iwaki General Hospital, Ohta Nishinouchi General Hospital, Takeda General Hospital, Tokyo Women's Medical University Daini Hospital, Saitama Medical School, Matsudo Municipal Hospital, Higashi Matsudo Hospital, Kameda General Hospital, Niigata University, Toyama Prefectural Central Hospital, Kanazawa University, Noto General Hospital, Nagano Municipal Hospital, Nagano Red Cross Hospital, Hamamatsu Medical Center, Inazawa Municipal Hospital, Aichi Prefectural Hospital, Toyota Memorial Hospital, Fujita Health University School of Medicine, Nishio Municipal Hospital, Toyohashi Municipal Hospital, Okazaki Municipal Hospital, Ichinomiya Municipal Hospital, Japanese Red Cross Nagoya First Hospital, Nagoya Memorial Hospital, Nagoya City University Medical School, Nagoya Ekisaikai Hospital, Aichi Cancer Center, Suzuka Chuo General Hospital, Suzuka Kaisei General Hospital, Mie University School of Medicine, Matsusaka Municipal Hospital, Matsusaka Chuo General Hospital, Matsusaka Saiseikai General Hospital, Yamada Red Cross Hospital, Ise Municipal General Hospital, Kyoto University, Kyoto Prefectural University of Medicine, Rinku General Medical Center, Okayama University Medical School, Okayama Saiseikai General Hospital, Chugoku Central Hospital of the Mutual Aid Association of Public School Teachers, Okayama Red Cross General Hospital, Fukuoka University School of Medicine, Kyushu Cancer Center, Kyushu University, and University of the Ryukyus.

Authorship and Disclosures

MY, NN, RS, TM, and SN contributed to the design of the study, provided clinical data and samples, analyzed the data, and wrote the manuscript. YK, MO, RI, TY, JS, TM, IM, KO, MN, JT, and MT provided clinical data and samples and critically reviewed the manuscript. MH, YM, RU, and HS provided clinical data and gave critical advice on the study to improve its intellectual content.

The authors reported no potential conflicts of interest.

References

1. Harris NL, Jaffe ES, Stein H, Banks PM, Chan JK, Cleary ML, et al. A revised European-American classification of lymphoid neoplasms: a proposal from the International Lymphoma Study Group. Blood 1994;84:1361-92.
2. Jaffe ES, Harris NL, Stein H, Vardiman JW. World Health Organization classification of tumours. Pathology and genetics of tumours of haematopoietic and lymphoid tissues. Lyon: IARC Press, 2001.
3. Matolcsy A, Chadburn A, Knowles DM. De novo CD5-positive and Richter's syndrome-associated diffuse large B cell lymphomas are genotypically distinct. Am J Pathol 1995; 147:207-16.
4. Yatabe Y, Nakamura S, Seto M, Kuroda H, Kagami Y, Suzuki R, et al. Clinicopathologic study of PRAD1/cyclin D1 overexpressing lymphoma with special reference to mantle cell lymphoma. A distinct molecular pathologic entity. Am J Surg Pathol 1996;20:1110-22.
5. Kume M, Suzuki R, Yatabe Y, Kagami Y, Miura I, Miura AB, et al. Somatic hypermutations in the VH segment of immunoglobulin genes of CD5-positive diffuse large B-cell lymphomas. Jpn J Cancer Res 1997;88: 1087-93.
6. Taniguchi M, Oka K, Hiasa A, Yamaguchi M, Ohno T, Kita K, et al. De novo CD5+ diffuse large B-cell lymphomas express VH genes with somatic mutation. Blood 1998;91: 1145-51.
7. Yamaguchi M, Ohno T, Oka K, Taniguchi M, Ito M, Kita K, et al. De novo CD5-positive diffuse large B-cell lymphoma: clinical characteristics and therapeutic outcome. Br J Haematol 1999;105:1133-9.
8. Nakamura N, Hashimoto Y, Kuze T, Tasaki K, Sasaki Y, Sato M, et al. Analysis of the immunoglobulin heavy chain gene variable region of CD5-positive diffuse large B-cell lymphoma. Lab Invest 1999;79:925-33.
9. Harada S, Suzuki R, Uehira K, Yatabe Y, Kagami Y, Ogura M, et al. Molecular and immunological dissection of diffuse large B cell lymphoma: CD5+, and CD5- with CD10+ groups may constitute clinically relevant subtypes. Leukemia 1999;13:1441-7.
10. Kroft SH, Howard MS, Picker LJ, Ansari MQ, Aquino DB, McKenna RW. De novo CD5+ diffuse large B-cell lymphomas. A heterogeneous group containing an unusual form of splenic lymphoma. Am J Clin Pathol 2000;114:523-33.

11. Yamaguchi M, Seto M, Okamoto M, Ichinohasama R, Nakamura N, Yoshino T, et al. De novo CD5+ diffuse large B-cell lymphoma: a clinicopathologic study of 109 patients. Blood 2002;99:815-21.
12. Kobayashi T, Yamaguchi M, Kim S, Morikawa J, Ogawa S, Ueno S, et al. Microarray reveals differences in both tumors and vascular specific gene expression in de novo CD5+ and CD5- diffuse large B-cell lymphomas. Cancer Res 2003;63:60-6.
13. Katzenberger T, Lohr A, Schwarz S, Dreyling M, Schoof J, Nickenig C, et al. Genetic analysis of de novo CD5+ diffuse large B-cell lymphomas suggests an origin from a somatically mutated CD5+ progenitor B cell. Blood 2003;101:699-702.
14. Kaman S, Tagawa H, Suzuki R, Suguro M, Yamaguchi M, Okamoto M, et al. Analysis of chromosomal imbalances in de novo CD5-positive diffuse large-B-cell lymphoma detected by comparative genomic hybridization. Gene Chromosomes Cancer 2004;39:77-81.
15. Tagawa H, Tsuzuki S, Suzuki R, Kaman S, Ota A, Kameoka Y, et al. Genome-wide array-based comparative genomic hybridization of diffuse large B-cell lymphoma: comparison between CD5-positive and CD5-negative cases. Cancer Res 2004;64: 5948-55.
16. Tagawa H, Suguro M, Tsuzuki S, Matsuo K, Kaman S, Ohshima K, et al. Comparison of genome profiles for identification of distinct subgroups of diffuse large B-cell lymphoma. Blood 2005;106:1770-7.
17. Suguro M, Tagawa H, Kagami Y, Okamoto M, Ohshima K, Shiku H, et al. Expression profiling analysis of the CD5+ diffuse large B-cell lymphoma subgroup: development of a CD5 signature. Cancer Sci 2006;97: 868-74.
18. Yoshioka T, Miura I, Kume M, Takahashi N, Okamoto M, Ichinohasama R, et al. Cytogenetic features of de novo CD5-positive diffuse large B-cell lymphoma: chromosome aberrations affecting 8p21 and 11q13 constitute major subgroups with different overall survival. Gene Chromosomes Cancer 2005;42:149-57.
19. Khalidi HS, Brynes RK, Browne P, Koo CH, Battifora H, Medeiros LJ. Intravascular large B-cell lymphoma: the CD5 antigen is expressed by a subset of cases. Mod Pathol 1998; 11:983-8.
20. Kanda M, Suzumiya J, Ohshima K, Tamura K, Kikuchi M. Intravascular large cell lymphoma: clinicopathological, immuno-histochemical and molecular genetic studies. Leuk Lymphoma 1999;34:569-80.
21. Murase T, Yamaguchi M, Suzuki R, Okamoto M, Sato Y, Tamaru JI, et al. Intravascular large B-cell lymphoma IVLBCL: a chnicopathologic study of 96 cases with special reference to the immunophenotypic heterogeneity of CD5. Blood 2007;109:478-85.
22. Ponzoni M, Ferreri AJ, Campo E, Facchetti F, Mazzucchelli L, Yoshino T, et al. Definition, diagnosis, and management of intravascular large B-cell lymphoma: proposals and perspectives from an international consensus meeting. J Clin Oncol 2007; 25:3168-73.
23. Chang CC, Bunyi-Teopengco E, Eshoa C, Chitambar CR, Kampalath B. CD5+ T-cell/histiocyte-rich large B-cell lymphoma. Mod Pathol 2002; 15:1051-7.
24. Barry TS, Jaffe ES, Kingma DW, Martin AW, Sorbara L, Raffeld M, et al. CD5+ follicular lymphoma: a clinicopathologic study of three cases. Am J Clin Pathol 2002;118:589-98.
25. Manazza AD, Bonello L, Pagano M, Chiusa L, Novero D, Stacchini A, et al. Follicular origin of a subset of CD5+diffuse large B-cell lymphomas. Am J Clin Pathol 2005;124:182-90.
26. Lin CW, O'Brien S, Faber J, Manshouri T, Romaguera J, Huh YO, et al. De novo CD5+ Burkitt lymphoma/leukemia. Am J Clin Pathol 1999;112:828-35.
27. Suzuki R, Yamamoto K, Seto M, Kagami Y, Ogura M, Yatabe Y, et al. CD7+ and CD56+ myeloid/natural killer cell precursor acute leukemia: a distinct hematolymphoid disease entity. Blood 1997;90:2417-28.
28. Yatabe Y, Suzuki R, Tobinai K, Matsuno Y, Ichinohasama R, Okamoto M, et al. Significance of cyclin D1 overexpression for the diagnosis of mantle cell lymphoma: a clinicopathologic comparison of cyclin D1-positive MCL and cyclin D1-negative MCL-like B-cell lymphoma. Blood 2000;95:2253-61.
29. Hermine O, Haioun C, Lepage E, d'Agay MF, Briere J, Lavignac C, et al. Prognostic significance of bcl-2 protein expression in aggressive non-Hodgkin's lymphoma. Groupe d'Etude des Lymphomes de l'Adulte GELA. Blood 1996;87:265-72.
30. Hans CP, Weisenburger DD, Greiner TC, Gascoyne RD, Delabie J, Ott G, et al. Confirmation of the molecular classification of diffuse large B-cell lymphoma by immunohistochemistry using a tissue microarray. Blood 2004;103:275-82.
31. A predictive model for aggressive non-Hodgkin's lymphoma. The International Non-Hodgkin's Lymphoma Prognostic Factors Project. N Engl J Med 1993;329:987-94.
32. Matolcsy A, Inghirami G, Knowles DM. Molecular genetic demonstration of the diverse evolution of Richter's syndrome (chronic lymphocytic leukemia and subsequent large cell lymphoma). Blood 1994; 83:1363-72.
33. The World Health Organization classification of malignant lymphomas in Japan: incidence of recently recognized entities. Lymphoma Study Group of Japanese Pathologists. Pathol Int 2000;50:696-702.
34. Tamura K, Sawada H, Izumi Y, Fukuda T, Utsunomiya A, Ikeda S, et al. Chronic lymphocytic leukemia CLL is rare, but the proportion of T-CLL is high in Japan. Eur J Haematol 2001;67:152-7.
35. Inaba T, Shimazaki C, Sumikuma T, Okano A, Hatsuse M, Okamoto A, et al. Expression of T-cell-associated antigens in B-cell non-Hodgkin's lymphoma. Br J Haematol 2000;109: 592-9.
36. Ogawa S, Yamaguchi M, Oka K, Taniguchi M, Ito M, Nishii K, et al. CD21S antigen expression in tumour cells of diffuse large B-cell lymphomas is an independent prognostic factor indicating better overall survival. Br J Haematol 2004;125:180-6.
37. Linderoth J, Jerkeman M, Cavallin-Stahl E, Kvaloy S, Torlakovic E. Immunohistochemical expression of CD23 and CD40 may identify prognostically favorable subgroups of diffuse large B-cell lymphoma: a Nordic Lymphoma Group study. Clin Cancer Res 2003;9:722-8.
38. Gary-Gouy H, Harriague J, Bismuth G, Platzer C, Schmitt C, Dalloul AH. Human CD5 promotes B-cell survival through stimulation of autocrine IL-10 production. Blood 2002;100:4537-43.
39. Mounier N, Briere J, Gisselbrecht C, Emile J-F, Lederlin P, Sebban C, et al. Rituximab plus CHOP R-CHOP overcomes bcl2-associated resistance to chemotherapy in elderly patients with diffuse large B-cell lymphoma DLBCL. Blood 2003; 101:4279-84.
40. Winter JN, Weller EA, Horning SJ, Krajewska M, Variakojis D, Habermann TM, et al. Prognostic significance of Bcl-6 protein expression in DLBCL treated with CHOP or R-CHOP: a prospective correlative study. Blood 2006;107:4207-13.
41. Nyman H, Adde M, Karjalainen-Lindsberg M-L, Taskinen M, Berglund M, Amini R-M, et al. Prognostic impact of immunohistochemically defined germinal center phenotype in diffuse large B-cell lymphoma patients treated with immunochemotherapy. Blood 2007; 109:4930-5.
42. Hollender A, Kvaloy S, Nome O, Skovlund E, Lote K, Holte H. Central nervous system involvement following diagnosis of non-Hodgkin's lymphoma: a risk model. Ann Oncol 2002;13:1099-107.
43. Feugier P, Virion JM, Tilly H, Haioun C, Marit G, Macro M, et al. Incidence and risk factors for central nervous system occurrence in elderly patients with diffuse large-B-cell lymphoma: influence of rituximab. Ann Oncol 2004;15:129-33.
44. Tilly H, Lepage E, Coiffier B, Blanc M, Herbrecht R, Bosly A, et al. Intensive conventional chemotherapy (ACVBP regimen) compared with standard CHOP for poor-prognosis aggressive non-Hodgkin lymphoma. Blood 2003;102:4284-9.

European Journal of Haematology ISSN 0902-4441

ORIGINAL ARTICLE

Immunoglobulin light chain gene translocations in non-Hodgkin's lymphoma as assessed by fluorescence *in situ* hybridisation

Yoshiko Fujimoto[1], Kenichi Nomura[1], Shuji Fukada[2], Daisuke Shimizu[1], Kazuho Shimura[1], Yosuke Matsumoto[1], Shigeo Horiike[1], Kazuhiro Nishida[1], Chihiro Shimazaki[1], Masafumi Abe[3], Masafumi Taniwaki[1,4]

[1]Department of Molecular Hematology and Oncology, Kyoto Prefectural University of Medicine, Graduate School of Medical Science, Kyoto, Japan; [2]Department of Internal Medicine, Kobe, Japan; [3]First Department of Pathology, School of Medicine, Fukushima Medical University, Fukushima, Japan; [4]Department of Molecular Cytogenetics and Laboratory Medicine, Kyoto Prefectural University of Medicine, Graduate School of Medical Science, Kyoto, Japan

Abstract

In non-Hodgkin's lymphoma (NHL), the majority of translocations involve the immunoglobulin heavy chain gene (*IGH*) locus, while a few involve the immunoglobulin light chain gene (*IGL*) locus, consisting of the kappa light chain gene (*IGκ*) and the lambda light chain gene (*IGλ*). Although many reports have dealt with the translocation and/or amplification of *IGH* in NHL, only a few have identified *IGL* translocations. To identify cytogenetic abnormalities and the partner chromosomes of *IGL* translocations in NHL, we performed dual-colour fluorescence *in situ* hybridisation (DC-FISH) and spectral karyotyping (SKY) in seven NHL cell lines and 40 patients with NHL. We detected *IGL* translocations in two cell lines and nine patients: four patients with diffuse large B-cell lymphoma, three with follicular lymphoma, one with extranodal marginal zone B-cell lymphoma of mucosa-associated lymphoid tissue and one with mantle cell lymphoma. Five distinct partners of *IGλ* translocation were identified by SKY analysis: 3q27 in three patients, and 1p13, 6p25, 17p11.2 and 17q21 in one patient each. Three cases featured double translocations of *IGH* and *IGL*. These findings warrant the identification of novel genes 1p13, 6p25, 17p11.2 and 17q21.

Key words immunoglobulin light chain gene; FISH; non-Hodgkin's lymphoma; double translocation

Correspondence Yoshiko Fujimoto, MD, Department of Molecular Hematology and Oncology, Kyoto Prefectural University of Medicine, Graduate School of Medical Science, Kawaramachi-Hirokoji, Kamigyo-ku, Kyoto 602-8566, Japan. Tel: +81-75-251-5740; Fax: +81-75-251-5743; e-mail: ysk-fjmt@koto.kpu-m.ac.jp

Accepted for publication 20 October 2007

doi:10.1111/j.1600-0609.2007.00993.x

A number of recurring chromosomal abnormalities correlate with clinical, morphological and immunophenotypic features of malignant lymphoma (1). The majority of these translocations involve the immunoglobulin heavy chain gene (*IGH*) locus, while a few involve the immunoglobulin light chain gene (*IGL*) locus, consisting of the kappa light chain gene (*IGκ*) located at 2p11.2 and the lambda light chain gene (*IGλ*) located at 22q11.2. The detection of these abnormalities, such as *IGH*, *IGλ* or *IGκ/C-MYC* translocations in Burkitt's lymphoma, can be useful for establishing and confirming diagnosis (2).

While previous reports have dealt with abnormalities of *IGH* translocation, including the double translocation and/or amplification of the C-region (3–5), those of *IGL* have been investigated to a much lesser extent. To identify the partner chromosome involved in the translocation and amplification of *IGL* in non-Hodgkin's lymphoma (NHL), we performed cytogenetic analysis using dual-colour fluorescence *in situ* hybridisation (DC-FISH) in seven NHL cell lines and 40 patients with B-cell NHL. We then corrected the molecular–cytogenetic findings with clinical findings in nine patients showing distinct partners of *IGL* translocation

to clarify whether *IGL* translocation is associated with a subset of NHL.

Patients and methods

Patients and clinical findings

Forty patients treated at the Kyoto Prefectural University of Medicine or Kuma Hospital (specialised hospital for thyroid disease) between April 2001 and March 2006, and seven cell lines established at the School of Medicine, Fukushima Medical University (HBL 1,2,3,5,6,8 and 9), were studied with FISH to identify *IGL* translocations by molecular cytogenetic methods. Clinical stages of NHL patients were defined according to the Ann Arbor staging classification (6), using staging procedures including physical examination, a routine laboratory profile, a chest radiograph and computed tomography scan. Tumour cells were analysed with a routine morphological review and immunophenotypic analysis. Histological subtypes were defined according to the World Health Organization (WHO) classification (1). The immunophenotype of tumour cells was assessed by flow cytometry or immunoperoxidase staining with L26 on paraffin-embedded sections according to the standard protocol (7).

Preparation of metaphase and interphase cells

Metaphase spreads and interphase nuclei were prepared from short-term cultures of lymph node tumour cells. Cells were treated with hypotonic solution of 0.075 M KCl at 20°C and fixed with Calnoy's solution [methanol : acetic acid (3 : 1)], as described previously (8). Control samples for interphase analysis were prepared from cultured lymph node cells from five patients with lymphadenitis. G-banded metaphases were arranged and defined according to the recommendations of the International System for Cytogenetic Nomenclature (2005) (9).

DC-FISH and SKY

For the detection of *IGL* translocation, we used bacterial artificial chromosome (BAC) clones purchased from Invitrogen Inc. (Carlsbad, CA, USA). FISH analysis was performed using differentially labelled probes flanking the *IGL* locus. Within the *IGλ* region, we selected the BAC clone RP11-1152K19 to cover the variable cluster (*IGλV*), and the BAC clone RP11-165G5 to cover the constant cluster (*IGλC*). Within the *IGκ* region, a clone (RP11-316G9) was selected to cover the variable cluster (*IGκV*), and a clone (RP11-1021F11) to cover the *IGκ* constant cluster (*IGκC*) (Fig. 1) (10, 11). For the detection of *IGH* translocations, *IGH* dual-colour breakpoint probes (Vysis, Burlingame, CA, USA) were used. For the detection of *BCL6* translocations, the LSI BCL6 (Vysis) probe was used. Each chromosome and nuclei were identified on the basis of 4′,6-diaminido-2-phenylindole dihydrochloride (DAPI) staining properties. Slides were mounted in an antifade solution (Vectashield; Vector Laboratories, Burlingame, CA, USA). Images were captured with a charge-coupled device (CCD) camera (SenSys0400-G1; Photometrics Ltd, Tucson, AZ, USA). For the analysis of

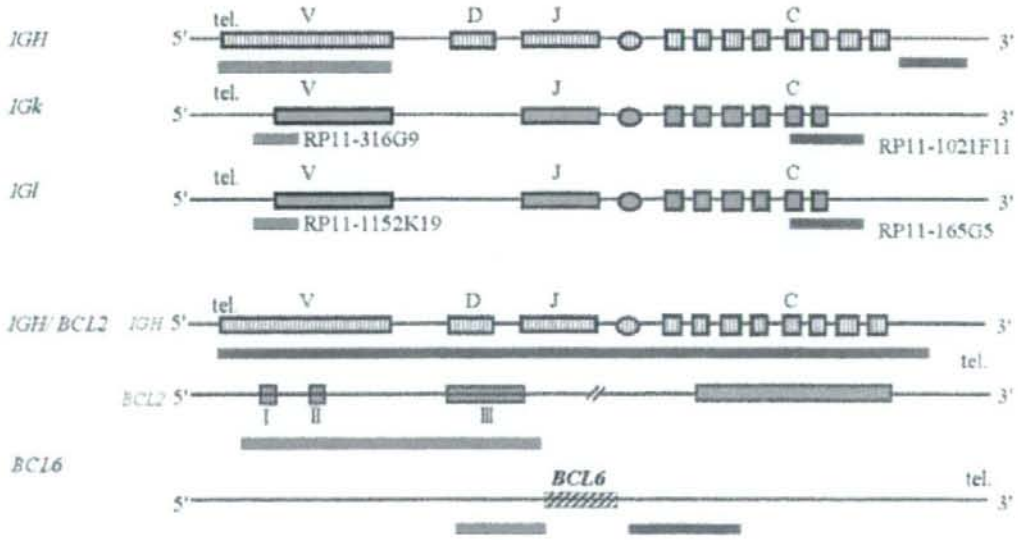

Figure 1 Schematic representation of probe locations for FISH analysis.

Table 1 Molecular–cytogenetic findings in nine patients with *IGL* translocation

Case no.	Chromosomal abnormalities	Materials	*IGL* translocation	Frequency of *IGL* split (%)	Partner of IGL translocation
1	add(22)(q11)	Lymph node	λ	50	17p11.2
2	t(2;3)(p12;q27),+del(3)(q?),der(3)t(2;3),+t(14;18)	Lymph node	κ	60	*BCL6*[1] and unknown
3	t(17;22)(q21;q11)	Lymph node	λ	80	17q21
4	t(3;22)(q27;q11)	Thyroid	λ	25	*BCL6*[1]
5	t(3;22)(q27;q11)	Thyroid	λ	86	*BCL6*[1]
6	t(6;22)(p25;q11)	Thyroid	λ	60	6p25
7	add(22)(q11)	Pancreas	λ	60	ND
8	add(22)(q11),+t(14;18)	Duodenum	λ	28	ND
9	t(1;2)(p13;p11),+2,add(4)(q21),+7,inv(9)(p11q13), t(14;18)(q32;q21)	Lymph node	κ	20	1p13
HBL2				80	
HBL6				92	

[1]Proved by FISH using the BCL6 split probe (Vysis).
ND, not defined.

Table 2 Representative karyotype by G-banding and spectral karyotyping analysis in two lymphoma cell lines and nine patients with B-cell lymphoma

Case	G-banding	Spectral karyotyping
HBL2	NA[1]	42,X,der(1)(1p12-1q42::?),der(3)(3pter-3q22;;15q15-15qter), dup(4)(p11p16), t(6;9)(q21;p13),del(7)(q11.1), der(8)t(8;?)(p23;?),t(11;14)(q13;q32), der(14)t(14,15)(q32.1;q15), der(15)t(8;15)(q24;q11.2), der(15)(?::15p11.1-15q13::3q22-3qter),−16, der(18)t(11;18)(q21;q11.2), der(18)(18pter-18q21.3::18q22.1-18q22.3::18q22.1-18q23::?), der(22)(9qter-9p12::22p11.1-22q11.2)[5/5]
HBL6	NA	44.t(X;6)(q28;q21), der(1)t(1;8)(p22;q24), der(2)t(1;2)(q32;q13), der(4)t(2;4)(p11.2;p12), −5,i(8q),der(9)t(9;20)(p13,p11.2), der(10)t(2;10)(p15;p15),der(10)t(5;10)(q31;q24), der(11)(11 pter-11q23::11q13-11q21::18q21-18qter),der(13)t(10,13)(q22;q34), dup(15)(q13q26), der(18)t(3;18)(q25;q21) [6/6]
No. 1	46,XY,add(7)(p11),add(17)(p11),add(22) (q11)[1/10]	45.XY,ins(7;13)(p15;q14q34),der(8)t(8;13)(p23.1;q?),del(13)(q14q34),+13, der(17)t(17;22)(p11.2;q11.2),−22[1/13]
No. 2	56,XX,add(1)(q21),t(2;3)(p12;q27), +del(3)(q?),der(3)t(2;3),+5,del(6)(q?),+7, +8,add(8)(p11)x2,+9,+9,+12,−13,t(14;18)(q32;q21), −15,−16,−17,+20,+der(?)t(?;1)(?;q12)x2,+mar1,+mar2, +mar3,+mar4 [2/7]	51,XX,der(1)t(1;3)(p12;?),der(1)t(1;8)(p36.1;p11.2),t(2;3)(p11.2;q27), +der(3)t(2;3),t(4;19)(q35;p13.1),+5,del(6)(q15q21), der(8)t(8;9)(p11.2;p13), der(9)t(6;9)(q13;p13),+der(11)t(11;17)(q13;q11.2),+12, der(14)t(14;21)(p11.2;q11.2),−15,der(17)(13qter-13q12::1::17p11. 2-17qter), der(18)t(8;18)(p11.2;p11.2),+20[1/4]
No. 3	48,XX,add(2)(p13),de1(2)(q?), add(6)(q21),de1(6)(q?),add(12)(p11), −14,t(17;22)(q21;q11),add(18)(q21), der(19)t(1;19)(q21;q13),add(20)(q11), +21,+der(?)t(?;14)(?;q11),+mar1 [15/20]	47,XX,t(2;6)(q23;q16),der(6)t(X;6)(q22;q26),del(11)(q13), t(12;14)(p11.1;p11.1),t(17;22)(q11.2;q11.2),der(16)t(16;18)(q24;q23), der(18)(18pter-18q21.3::18q21.1-18q23::16qter), der(19)t(1;19)(q21;q13.4),+der(19)t(1;19)(p12;p11), ?tul=1>der(20)t(11;20)(q13;11.2) [3/5]
No. 4	46,XX,t(3;22)(q27;q11),add(7)(q32), t(14;18)(q32;q21),der(16)t(1;16)(q21;q22) [1/15]	NA[1]
No. 5	46,XX,t(3;22)(q27;q11) [15/20]	NA
No. 6	46,XX,t(6;22)(p25;q11)[5/7]	NA
No. 7	46,XY,add(8)(p11),add(20)(q13),add(22)(q11) [2/20]	46XY,t(8:22)(p11;q11.2) [1/20]
No. 8	46,XY,add(10)(q11),t(14;18)(q32;q21) [12/20] 46,idem,add(22)(q11) [5/20]	46,XY,del(10)(q11;q24),t(14;18)(q32;q21) [3/20]
No. 9	48,XY,t(1;2)(p13;p11),+2,add(4)(q21),+7,inv(9)(p11q13), t(14;18)(q32;q21) [2/20]	NA

[1]NA, not available.

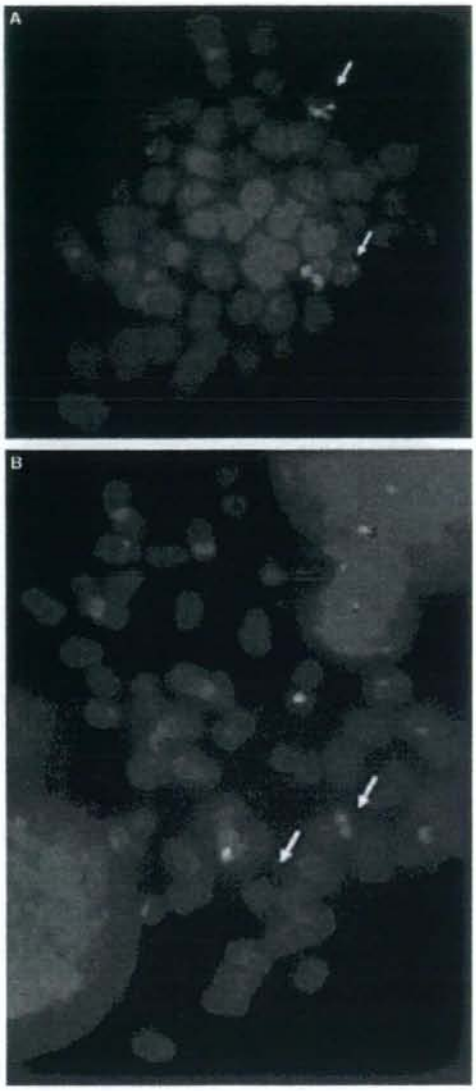

Figure 2 (A) DC-FISH showing *IGH/BCL2* translocation. Green and orange signals identify *IGH* and *BCL2*, respectively. Fusion signals indicated by arrows suggest *IGH/BCL2* translocation. (B) DC-FISH showing *IGH* translocation. Split signals of *IGHC* (red) and *IGHV* (green) indicate that the breakpoint is located between variable and constant regions.

non-dividing cells, hybridisation signals were evaluated in 100 interphase nuclei per slide. The split signals of the *IGL* gene and those of LSI BCL6 probes were defined based on the cut-off values which were calculated from the mean + 2SD, as reported previously (12, 13). Spectral

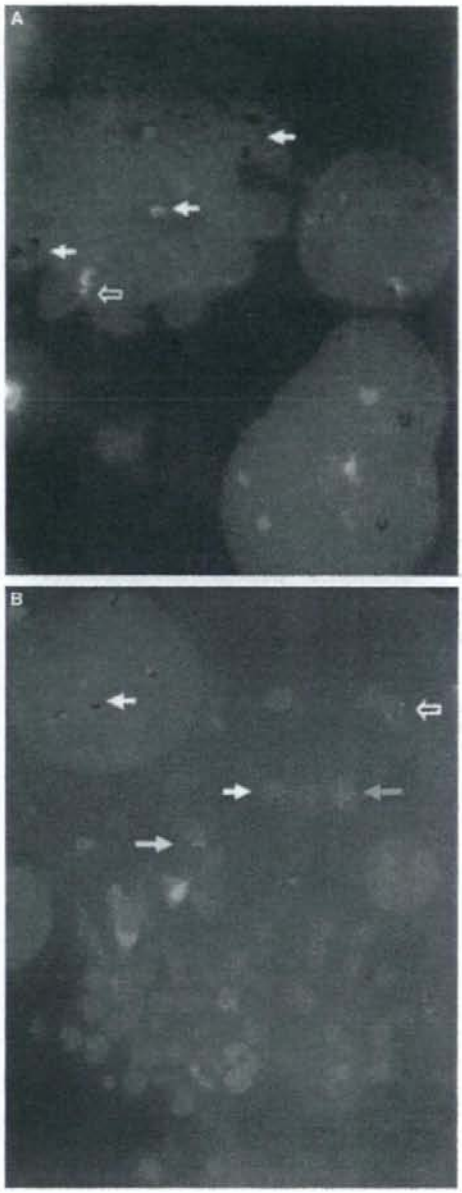

Figure 3 (A) FISH showing *IGκ* translocation. The open arrow indicates the normal *IGκ* gene. Closed arrows indicate a split signal. (B) FISH showing *BCL6* translocation. The open arrow indicates a telomeric probe showing up as red on der(3)t(2;3). Closed, yellow and blue arrows indicate the abnormal chromosome of der(2)t(2;3)(p11.2;q27), normal chromosome 3 and der(1)t(1;3)(p12;7), respectively. The green signal expected to be on der(3)t(2;3) is not detected.

karyotyping (SKY) was carried out with a SkyPaint kit (Applied Spectral Imaging, Migdal Ha'Emek, Israel). Signal detection was performed according to the manufacturer's instructions.

Results

FISH and SKY analyses of patients and cell lines

Nine cases of 2p11 or 22q11 rearrangements were diagnosed as having *IGL* translocations based on FISH findings. The frequency of *IGL* translocation-positive cells ranged from 20% to 86% (Table 1). There were two cases of *IGκ* translocation and seven of *IGλ* translocation. Distinct partners were defined as *BCL6* in three cases of *IGL* translocation and as 1p13, 6p25, 17p11.2 and 17q21 in one case each. Cut-off values were defined according to the mean ± 2SD: 5.3 ± 0.8% for split signals in *IGL* translocation and 4.2 ± 1.0% for split signals in t(3;22) translocation. Cytogenetic findings of these nine patients are summarised in Table 2. G-banding analysis identified t(3;22) in two patients (no. 4 and 5), t(2;3) in patient no.2, and t(17;22)(q21;q11) in patient no. 3. Patients no. 2, 8 and 9 showed t(14;18)(q32;q21) in addition to t(2;3) or add(22)(q11).

Figure 3 shows the FISH results in patient no. 2. The *BCL2/IGH* fusion signal was also identified on chromosome 14 by means of FISH in patient no. 2 (Fig. 2). One fused dual-colour signal for *IGκ* was supposed to be located on chromosome 2 (intact *IGκ* locus). Two isolated green signals (*IGκC*) and a single orange signal (*IGκV*) were detected on der(2)t(2;3)(p11.2;q27) and der(3)t(2;3), and der(2)t(2;3)(p11.2;q27) respectively (Fig. 3A). In this patient, *BCL6* translocation was identified with the *BCL6*-specific probe; one of the split signals was detected on der(2)t(2;3)(p11.2;q27). The split signal, which has to be identified as a green signal, located on t(2;3)(p11.2;q27) was supposed to be diminished on translocation (Fig. 3B). As shown in Fig. 4, SKY analysis identified t(2;3)(p11.2;q27), +der(3)t(2;3)(?;?) and +t(14;18)(q32;q21) in patient no.2 (Fig. 4). The results of FISH analysis together with SKY and G-banding analyses indicated that the *IGκC* region is amplified and then translocated to chromosome 3. Of the seven cell lines, FISH showed that two had undergone *IGL* translocation with a diminished *IGλV* signal, suggesting either physiological detection according to VJ recombination or an alternative mechanism that may be involved in generating these cell lines (Figs 5 and 6).

Clinical characteristics of patients with *IGL* translocation

Table 3 shows the clinical and histological findings of the nine patients with *IGL* translocation. Their ages ranged from 52 to 77 years, with a median of 65 years. One patient showed involvement of the central nervous system. Therapeutic outcomes were a complete response (CR) in eight patients, and partial response in the remaining one patient. Of the nine

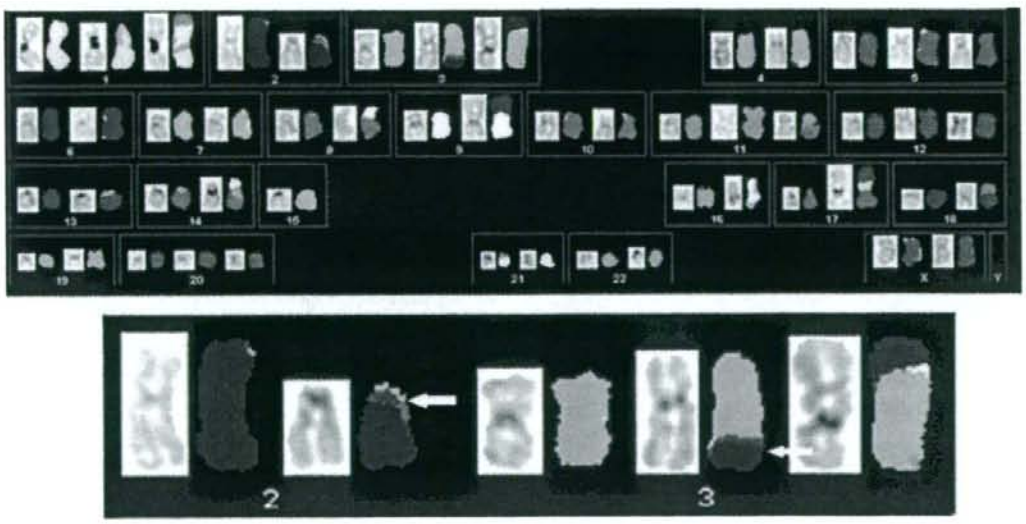

Figure 4 SKY analysis of patient no.2. Partial karyotypes, t(2;3)(p11.2;q27) and der(3)t(2;3)(?;?), are shown in the lower column. Arrows indicate the breakpoint of t(2;3)(p11.2;q27), each showing 2p11.2 and 3q27.

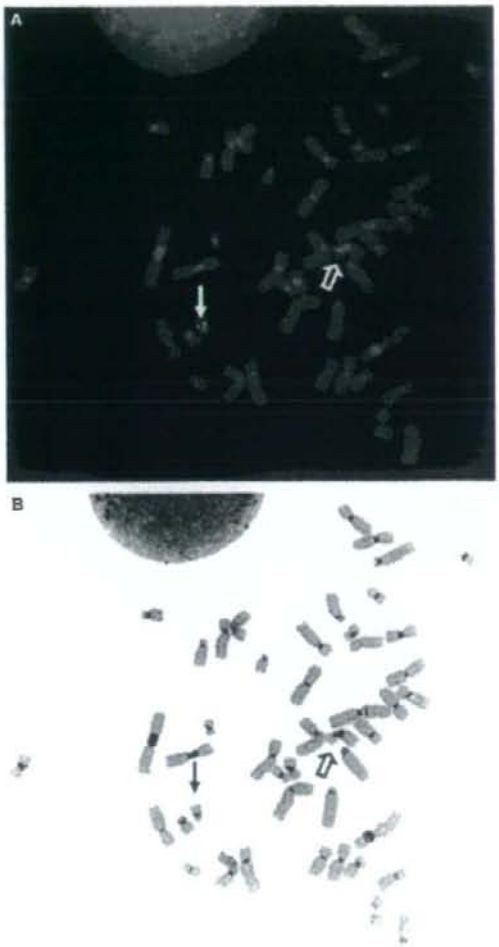

Figure 5 DC-FISH with the *IGλ* probe in the cell line HBL2. Red and green signals are originating from RP11-1152K19 and RP11-165G5, respectively. The green signal (open arrow) was detected on der(22). No red signal was detected, possibly due to the physiological VJ rearrangement of the *IGL* gene. (B) DAPI staining.

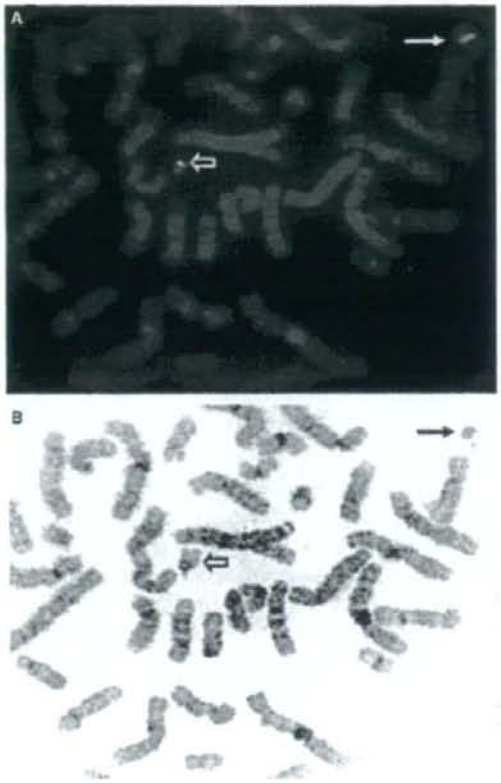

Figure 6 (A) DC-FISH with the *IGλ* probe in the lymphoma cell line HBL6. A fusion signal was detected on normal chromosome 22, as indicated by the open arrow. Only a green signal was noted on der(22), as indicated by the arrow. No V-region (red signal) was detected. (B) DAPI staining.

patients, seven were female and two were male. The histological subtypes of NHL were diffuse large B-cell lymphoma (DLBCL) in four patients, follicular lymphoma (FL) grade 2 in three patients, extranodal marginal zone B-cell lymphoma of mucosa-associated lymphoid tissue in one patient, and mantle cell lymphoma in one patient. Surface light chains were identified in all samples, and seven patients showed kappa light chain expression.

Discussion

IGL translocation was detected in two of seven cell lines and nine of 40 patients with B-cell lymphoma. We demonstrated two significant findings in this study. First, *IGL* and/or *IGH* double translocation was detected in three of 40 patients, accounting for 7.5% of B-cell lymphoma cases. Secondly, we identified novel translocation partners of *IGL* translocations in four patients. There have been a number of previous reports describing cases of double *IGH* translocation, or that of both *IGH* and *IGL* in B-cell malignancies (14–23). However, double *IGL* translocation has not been reported until now. Our case was identified as having double *IGL* translocation only through the use of FISH, indicating that FISH should be recommended for the detection of double *IGL* translocations, because the polymerase chain reaction

Table 3 Clinical and histological findings in nine patients with *IGL* translocation

Case no.	Age/Gender	Diagnosis	Surface light chain	Chemotherapy	Response	Survival (mo)
1	63/M	MCL	λ	R-CHO	PR	24
2	65/F	FL	λ	R-CHOP	CR	36+
3	52/F	DLBCL	κ	R-CHOP+Hi-MTX	CR	30+
4	64/F	DLBCL	κ	R-CHOP	CR	41+
5	68/F	MALT lymphoma	κ	R-CHOP	CR	40+
6	77/F	DLBCL	κ	R-CHOP	CR	17+
7	76/M	DLBCL	κ	R-CHOP	CR	6+
8	64/F	FL	κ	R-CHOP	CR	26+
9	73/F	FL	κ	R-CHOP	CR	51+

MCL, mantle cell lymphoma; FL, follicular lymphoma; MALT lymphoma, extranodal marginal zone B-cell lymphoma of mucosa-associated lymphoid tissue; DLBCL, diffuse large B-cell lymphoma; CR, complete response; PR, partial response; LN, lymph node; Hi-MTX, high-dose methotrexate.

method is not able to detect double *IGL* translocation with an unknown partner.

Regarding previous reports, the most frequent partner gene of *IGH* translocation is *BCL2*, while that of *IGL* is *c-MYC*. *c-MYC* has been supposed to be implicated in tumour progression such as the development from FL carrying t(14;18) to Burkitt's or Burkitt-like lymphoma (15, 16, 24–31). In these previous reports, tumour progression is possibly associated with the co-existence of *c-MYC* and *BCL2*, but not with the co-existence of translocations of *IGH* and *IGL*. FISH with the *IGL/c-MYC* probe may possibly predict the therapeutic response and prognosis.

We identified chromosomal bands 1p13, 6p25, 17p11.2 and 17q21 as partners in *IGL* translocation. Although these breakpoints should be narrowed down by FISH specific for each locus-band probe to identify candidate genes located in these loci, samples are not available for further studies because of the small sample size. Cell lines exhibiting these abnormalities will be required for identifying genes involved in *IGL* translocation associated with the development as well as progression of lymphoma.

Histologically, four and three of the nine patients showed DLBCL and FL subtypes, respectively. Regarding the clinical outcome, eight of nine patients achieved a CR with a cyclophosphamide, hydroxydaunorubicin, Oncovin, prednisolone (CHOP)-like regimen. *IGL/BCL6* translocation cases in our study are compatible with those of a previous study in terms of the clinical outcome, confirming that patients with *non-IG/BCL6* tend to show a poorer clinical outcome than those with *IG/BCL6* (32). In the current study, *IGL* translocation was associated with neither a histological nor clinical subtype of NHL, although further studies involving a large number of patients will be required to draw definitive conclusions.

In conclusion, FISH analysis suggests that *IGL* translocation may be associated with lymphoma development, although *IGL* and/or *IGH* translocation was not correlated with a specific subtype of NHL in the current study. The cytogenetic findings described herein warrant the identification of novel genes as partners of *IGL* translocation associated with lymphomagenesis.

Acknowledgements

We thank Miss Minako Gotoh and Kayoko Kurita for their technical assistance.

References

1. Harris NL, Jaffe ES, Diebold J, Flandrin G, Muller-Hermelink HK, Vardiman J. World Health Organization classification of neoplastic diseases of the hematopoietic and lymphoid tissues: report of the Clinical Advisory Committee meeting - Airlie House, Virginia. *J Clin Oncol* 1999;**17**:3835–49.
2. Willis TG, Dyer MJS. The role of immunoglobulin translocations in the pathogenesis of B-cell malignancies. *Blood* 1999;**96**:808–22.
3. Taniwaki M, Nishida K, Ueda Y, Misawa S, Nagai M, Tagawa S, Yamagami T, Sugiyama H, Abe M, Fukuhara S. Interphase and metaphase detection of the breakpoint of 14q32 translocations in B-cell malignancies by double-color fluorescence in situ hybridization. *Blood* 1995;**85**:3223–8.
4. Kanda-Akano Y, Nomura K, Fujita Y, *et al.* Molecular-cytogenetic characterization of non-Hodgkin's lymphoma with double and cryptic translocations of the immunoglobulin heavy chain gene. *Leuk Lymphoma* 2004;**45**:1559–67.
5. Nomura K, Kanda-Akano Y, Shimizu D, *et al.* An additional segment at 1p36 derived from der(18)t(14;18) in patients with diffuse large B-cell lymphomas transformed from follicular lymphoma. *Ann Haematol* 2005;**84**:474–6.
6. Carbone PP, Kaplan HS, Musshoff K, Smithers DW, Tubiana M. Report of the Committee on Hodgkin's Disease Staging Classification. *Cancer Res* 1971;**31**:1860–1.

7. Elghetany MT, Kurec AS, Schuehler K, Forbes BA, Duggan DB, Davey FR. Immunophenotyping of non-Hodgkin's lymphomas in paraffin-embedded tissue sections. A comparison with genotypic analysis. *Am J Clin Pathol* 1991;**95**:517–25.
8. Taniwaki M, Matsuda F, Jauch A, Nishida K, Takashima T, Tagawa S, Sugiyama H, Misawa S, Abe T, Kashima K. Detection of 14q32 translocations in B-cell malignancies by in situ hybridization with yeast artificial chromosome clones containing the human IgH gene locus. *Blood* 1994;**83**:2962–9.
9. ISCN. An International System for Human Cytogenetic Nomenclature. In: Shaffer LG, Tommerup N, eds. *Recommendations of the International Standing Comittee on Human Cytogenetic Nomenclature*. Basel: Karger, 2005.
10. Martin-Subero JI, Harder L, Gesk S, Schlegelberger B, Grote W, Martinez-Climent JA, Dyer MJ, Novo FJ, Calasanz MJ, Siebert R. Interphase FISH assays for the detection of translocations with breakpoints in immunoglobulin light chain loci. *Int J Cancer* 2002;**98**:470–4.
11. Poulsen TS, Silahtaroglu AN. Detection of illegitimate rearrangements within the immunoglobulin light chain loci in B cell malignancies using end-sequenced probes. *Leukemia* 2002;**16**:2156–8.
12. Iida S, Rao PH, Nallasivam P, Hibshoosh H, Butler M, Louie DC. The t(9;14)(p13;q32) chromosomal translocation associated with lymphoplasmacytoid lymphoma involves the PAX-5 gene. *Blood* 1996;**88**:4110–7.
13. Tamura A, Miura I, Iida S, Yokota S, Horiike S, Nishida K. Interphase detection of immunoglobulin heavy chain gene translocations with specific oncogene loci in 173 patients with B-cell lymphoma. *Cancer Genet Cytogenet* 2001;**29**:1–9.
14. D'Achille P, Seymour JF, Campbell LJ. Translocation (14;18)(q32;q21) in acute lymphoblastic leukemia: a study of 12 cases and review of the literature. *Cancer Genet Cytogenet* 2006;**171**:52–6.
15. De Jong D, Voetdijk BM, Beverstock GC, van Ommen GJ, Willemze R, Kluin PM. Activation of the c-myc oncogene in a precursor-B-cell blast crisis of follicular lymphoma, presenting as composite lymphoma. *N Engl J Med* 1988;**318**:1373–8.
16. Thangavelu M, Olopade O, Beckman E, Vardiman JW, Larson RA, McKeithan TW, Le Beau MM, Rowley JD. Clinical, morphologic, and cytogenetic characteristics of patients with lymphoid malignancies characterized by both t(14;18)(q32;q21) and t(8;14)(q24;q32) or t(8;22)(q24;q11). *Genes Chromosomes Cancer* 1990;**2**:147–58.
17. Koduru PR, Offit K. Molecular structure of double reciprocal translocations: significance in B-cell lymphomagenesis. *Oncogene* 1991;**6**:145–8.
18. Hebert J, Romana SP, Hillion J, Kerkaert JP, Bastard C, Berger R. Translocation t(3;22)(q27;q11) in non-Hodgkin's malignant lymphoma: chromosome painting and molecular studies. *Leukemia* 1993;**7**:1971–4.
19. Karsan A, Gascoyne RD, Coupland RW, Shepherd JD, Phillips GL, Horsman DE. Combination of t(14;18) and a Burkitt's type translocation in B-cell malignancies. *Leuk Lymphoma* 1993;**10**:433–41.
20. Berger R, Flexor M, Le Coniat M, Larsen CJ. Presence of three recurrent chromosomal reaarrangements, t(2;3)(p12;q37), del(8)(q24), and t(14;18), in an acute lymphoblastic leukemia. *Cancer Genet Cytogenet* 1996;**86**:76–9.
21. Fujii S, Miyata A, Takeuchi M, Yoshino T. Acute lymphoblastic leukemia (L3) with t(2;3)(p12;q27), t(14;18)(q32;q21), and t(8;22)(q24;q11). *Rinsho Ketsueki* 2005;**46**:134–40.
22. Bentley G, Palutke M, Mohamed AN. Variant t(14;18) in malignant lymphoma: a report of seven cases. *Cancer Genet Cytogenet* 2005;**157**:12–7.
23. Küppers R, Dalla-Favera R. Mechanisms of chromosomal translocations in B cell lymphomas. *Oncogene* 2001;**20**:5580–94.
24. Aventin A, Mecucci C, Guanyabens C, Brunet S, Soler J, Bordes R, van den Berghe H. Variant t(2;18) translocation in a Burkitt conversion of follicular lymphoma. *Br J Haematol* 1990;**4**:367–9.
25. Macpherson N, Lesack D, Klasa R, Horsman D, Connors JM, Barnett M, Gascoyne RD. Small noncleaved, non-Burkitt's (Burkit-Like) lymphoma: cytogenetics predict outcome and reflect clinical presentation. *J Clin Oncol* 1999;**17**:1558–67.
26. Klein G. Comparative action of myc and bcl-2 in B-cell malignancy. *Cancer Cells* 1991;**3**:141–3.
27. McDonnell TJ, Korsmeyer SJ. Progression from lymphoid hyperplasia to high-grade malignant lymphoma in mice transgenic for the t(14;18). *Nature* 1991;**349**:254–6.
28. Höglund M, Sehn L, Connors JM, Gascoyne RD, Siebert R, Säll T, Mitelman F, Horsman DE. Identification of cytogenetic subgroups and karyotypic pathways of clonal evolution in follicular lymphomas. *Genes Chromosomes Cancer* 2004;**39**:195–204.
29. Lee JT, Innes DJ Jr, Williams ME. Sequential bcl-2 and c-myc oncogene rearrangements associated with the clinical transformation of non-Hodgkin's lymphoma. *J Clin Invest* 1989;**84**:1454–9.
30. Yano T, Jaffe ES, Longo DL, Raffeld M. MYC rearrangements in histologically progressed follicular lymphomas. *Blood* 1992;**80**:758–67.
31. Martín-Subero JI, Odero MD, Hernandez R, *et al.* Amplification of IGH/MYC fusion in clinically aggressive IGH/BCL2-positive germinal center B-cell lymphomas. *Genes Chromosomes Cancer* 2005;**43**:414–23.
32. Akasaka T, Akasaka H, Ueda C, Yonetani N, Maesako Y, Shimizu A. Molecular and clinical features of non-Burkitt's, diffuse large-cell lymphoma of B-cell type associated with the c-MYC/immunoglobulin heavy-chain fusion gene. *J Clin Oncol* 2000;**18**:510–8.

ELSEVIER

Cancer Genetics and Cytogenetics 186 (2008) 54–57

CANCER GENETICS AND CYTOGENETICS

Short communication

Cytogenetic abnormality 46,XX,add(21)(q11.2) in a patient with follicular dendritic cell sarcoma

Naomi Suzuki[a], Hiroki Katsusihma[a], Kengo Takeuchi[b], Shigeo Nakamura[c], Kenichi Ishizawa[d], Seiichi Ishii[e], Takuya Moriya[f], John F. DeCoteau[g], Ikuo Miura[h], Ryo Ichinohasama[d,*]

[a]*Medical student, Tohoku University School of Medicine, Sendai, Japan*
[b]*Department of Pathology, Cancer Institute Hospital, Tokyo, Japan*
[c]*Department of Pathology and Clinical Laboratories, Nagoya University Hospital, Nagoya, Japan*
[d]*Division of Hematopathology, Tohoku University Graduate School of Medicine, 1-1 Seiryo-machi, Aoba-ku, Sendai 980-8574, Japan*
[e]*Department of Surgery, Tohoku University Graduate School of Medicine, Sendai, Japan*
[f]*Second Department of Pathology, Kawasaki Medical University*
[g]*Department of Pathology, University of Saskatchewan, Saskatoon Cancer Centre, Saskatoon, Canada*
[h]*Division of Hematology and Oncology, St. Marianna University School of Medicine, Kawasaki, Japan*

Received 25 March 2008; received in revised form 27 May 2008; accepted 5 June 2008

Abstract The case of a patient with follicular dendritic cell (FDC) sarcoma with chromosomal aberration add(21)(q11.2) is described. Cytogenetic studies showed the karyotype 46,XX,add(21)(q11.2)[3]/46,XX[17], although the encoded protein involved was not clarified. The abnormal pattern was quite simple, and different from a previous report. The clinical course of the FDC sarcoma in this case has been indolent, as for most FDC sarcoma patients. Although this patient suffered from breast carcinoma 6 years after the onset of FDC sarcoma, the carcinoma showed different histological and phenotypic profiles.

1. Introduction

Follicular dendritic cell (FDC) sarcoma is a rare neoplasm derived from FDCs, which normally form a tight meshwork in the primary and secondary lymphoid follicles and participate in the immune system by interacting with B or T lymphocytes [1,2]. The FDC sarcomas exhibit unique histological immunophenotypic features [3,4].

Although some 70 cases of FDC sarcomas have been reported in English literature to date [5], the definition of FDC sarcoma remains unclear—in part because FDCs may not comprise a single population. In addition, purification and detailed characterization of FDCs is very difficult due to their very small numbers. There has been no previous report of cytogenetic abnormalities occurring in FDC sarcoma. There is one report of a chromosomal aberration occurring in abnormal FDC-like stromal cells observed in Castleman disease [6,7], but this tumor can be considered distinct from FDC sarcoma. Here, we report a novel karyotypic abnormality in FDC sarcoma.

2. Case report

A 63-year-old Japanese woman noticed a lymph node swelling, up to 3 cm in diameter, in the region of the right axilla, in March 1994. Her medical history was notable only for tubal ligation for the purpose of contraception, and she had no specific family history. In another hospital, a needle core biopsy was performed and adenocarcinoma was suspected; however, no primary tumor site was identified and extensive physical examination, ultrasonography, and mammography of both breasts also showed no tumorous lesion.

The patient was transferred to our hospital and cytological examination revealed the presence of a lymphoid neoplasm, not carcinoma. Excisional biopsy of the same site was performed in April 1994, and a diagnosis of undifferentiated carcinoma was made because Hodgkin/RS cells were not found histologically and the neoplastic cells were negative for CD15 and CD30. Again, no other tumor site was identified, despite extensive examination including computed tomography, ultrasonography, mammography, and gastrointestinal endoscopy.

One year later, the tumor mass again became palpable at the same region. No abnormalities in the laboratory data were identified except for a slight increase of serum lactate

* Corresponding author. Tel.: +81-22-717-8238; fax: +81-22-717-8239.
E-mail address: ryo@mail.tains.tohoku.ac.jp (R. Ichinohasama).

0165-4608/08/$ – see front matter
doi:10.1016/j.cancergencyto.2008.06.002

dehydrogenase (414 U/L) and CA19-9 (40 U/mL). All enlarged lymph nodes were dissected; the tumorous lymph nodes were of soft elastic consistency, with the cut surfaces somewhat translucent and watery, similar to that of non-Hodgkin lymphoma.

Histological examination of the right axillary lymph node showed mainly a nodular or solid growth pattern resembling islands (Fig. 1A). In some areas, a partly storiform-like sarcomatous proliferation pattern was present, suggesting the so-called biphase feature. The neoplastic cells were often intimately admixed with abundant lymphocytes. No necrosis or glandular differentiation was identified in any tumorous component. The cell borders were indistinct, and the nuclei were round to oval with open chromatin and distinct small nucleoli (Fig.1B). Electron microscopic examination revealed occasional mature desmosome structures between tumor cells (Fig. 1C) and frequent opposed cytoplasmic processes (Fig. 1D), which were thin and sometimes long.

Immunohistochemical study of the tumor cells revealed an immunophenotype as follows: CD1a$^-$, CD3$^-$, CD4$^+$ (partly), CD8$^-$, CD15$^-$, CD21$^-$, CD23$^+$(partly), CD30$^-$, CD34$^-$, CD43$^-$, CD45RO$^-$, CD56$^-$, CD68$^-$, CD79a$^-$, DAKO-FDC$^+$, Ki-M1 p$^-$, HLA-DR$^+$, S100$\alpha\pm$, S100β^-, α-actin$^-$, desmin$^-$, vimentin$^+$, cytoplasmic epithelial membrane antigen(cEMA)$^+$, lysozyme$^-$, AE1/AE3$^+$, ER$^-$, PR$^-$, CK7$^-$, CD20$^-$, TIA-1$^-$, and granzyme B$^-$ on paraffin sections and CD35$^+$, Ki-M4$^-$, DRC-1$^-$, and R4/23$^-$ on

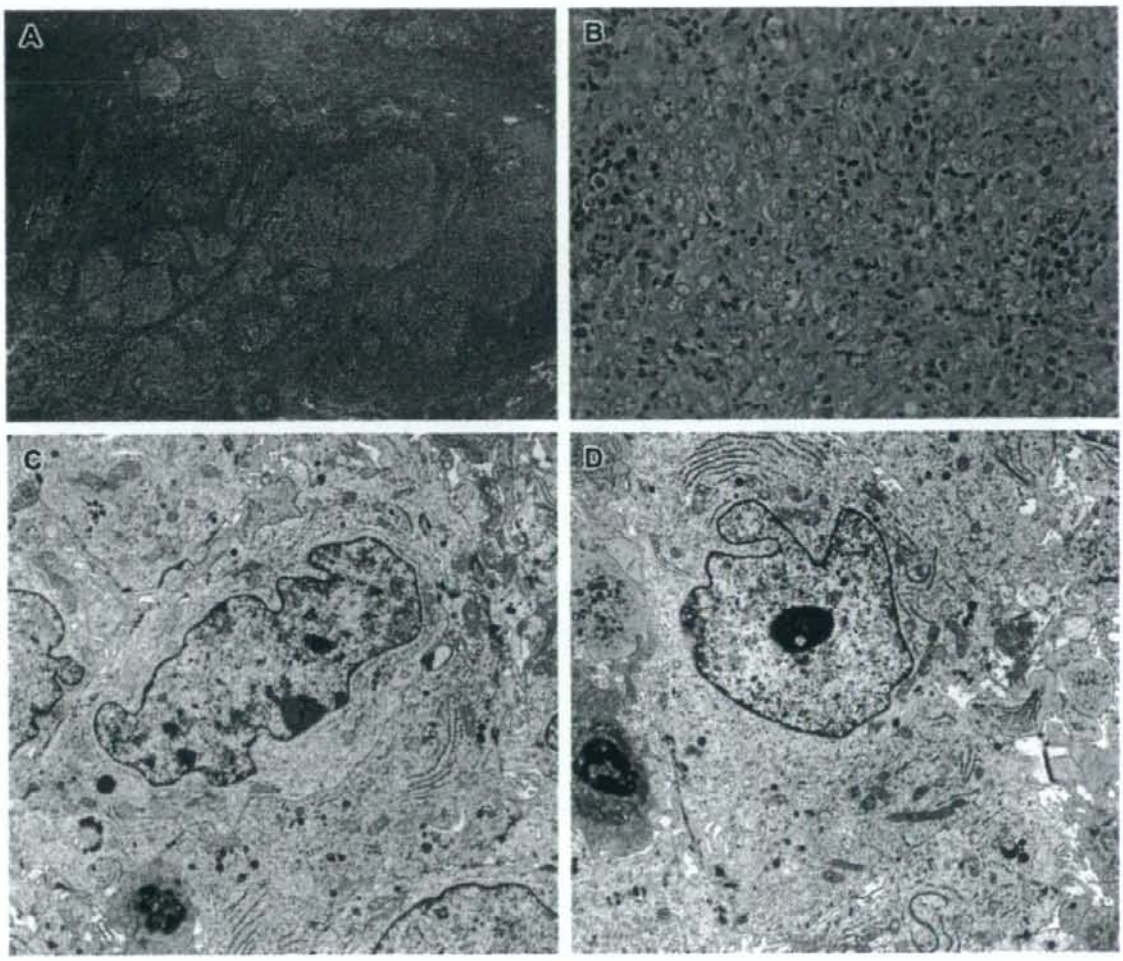

Fig. 1. (A) Low-power view of the follicular dendritic cell (FDC) sarcoma. The tumor shows solid and nodular growth pattern resembling islands. (B) High-power view of FDC sarcoma cells. The cell borders were indistinct, and the nuclei were round to oval, with open chromatin and distinct small nucleoli. (C) Electron microscopic image between neoplastic cells. FDC sarcoma cells have occasional mature desmosome structures between them. (D) Electron microscopic image of neoplastic cells. In part, surfaces of the FDC sarcoma cells exhibit frequent opposed cytoplasmic processes, thin and sometimes long.

frozen sections. No abnormal cell population was identified by flow cytometry, and Southern blot analysis showed germline configuration using the probes for both immunoglobulin heavy chain gene and T-cell receptor beta chain gene.

Based on these characteristic histological, immunohistochemical, and ultrastructural features, a diagnosis of FDC sarcoma was made. Although positive for CD23, CD35, and DAKO-FDC, the tumor was considered to be an immature variant, because of CD21 negativity.

Chromosome studies of the tumor were performed on 20 cells. With the suspended cells obtained from the biopsied lymph nodes, a sole cytogenetic abnormality was identified in 3 of 20 metaphases examined: 46,XX,add(21)(q11.2)[3]/46,XX[17] (Fig. 2).

The patient was completely disease free at any body site, including breasts and both axillae, for 6 years after the initial onset of lymph node swelling; however, a right breast mass was detected in March 2000. The diagnosis of ductal adenocarcinoma, class 5, was made based on aspiration cytology. Total mastectomy of the right breast was then performed, and the diagnosis of invasive ductal carcinoma, scirrhous, was made. No carcinoma metastases were present in the lymph nodes dissected at the mastectomy. The histological appearance and immunophenotype of the breast cancer was different from that of original tumor of the lymph nodes, thereby excluding metastases of occult breast cancer in the previously biopsied lymph node lesions.

After the breast surgery, the patient received 7 cycles of taxotere administration only, resulting in progressive disease. In 2002, the patient had multiple metastasis of carcinoma to the lymph nodes and skin and received 1 cycle of cyclophosphamide, adriamycin, and 5FU as well as irradiation to neck, mediastinum, and both axillae. She died of bilateral carcinomatous pleuritis in September 2002.

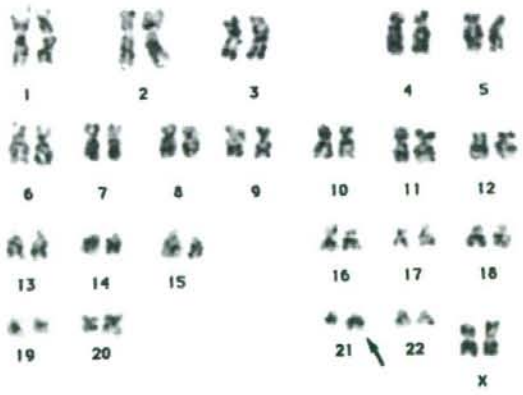

Fig. 2. Clonal chromosomal abnormality in a follicular dendritic cell sarcoma. G-banded metaphase analysis revealed a 46,XX,add(21)(q11.2)[3]/46,XX[17] karyotype.

3. Discussion

In general, there are many antigens positive for tumor cells of FDC sarcoma [8], and FDC sarcoma is said to be characterized by the expression of at least one FDC marker (e.g., CD21, CD35, R4/23 [4], CD23 [9], and DRC-1 [10]). The immunophenotypic results in our case—that is, positive CD35 and CD23, although partial—support the diagnosis of FDC sarcoma, along with the typical electron microscopic findings such as frequent dendritic processes of tumor cell surface and occasional desmosomes between tumor cells. In addition to these findings, positivity of DAKO-FDC on tumor cells may also be suggestive for the diagnosis of FDC sarcoma, although the evaluation of this antigen may be somewhat controversial, in that it is not included in the cluster differentiation (CD) classification. Of note, DAKO-FDC was negative in the breast carcinoma from this same patient.

In the present case, the FDC sarcoma cells were found to be negative for CD21. There are several reports of FDC sarcoma negative for CD21, and according to one report CD21 may be positive for mature FDCs [3,11,12]. Another report mentions that CD21 is negative in neoplastic cells derived from cells having characteristics of both FDCs and fibroblastic reticular cells [13]. We conclude that the FDC sarcoma in this study might be derived from more immature FDC.

Occult breast carcinoma has been reported [14], but we conclude that the breast carcinoma in the present case represents a distinct tumor for the following reasons: (i) there was a 6-year interval between the initial onset of FDC sarcoma and the breast carcinoma; (ii) the breast carcinoma contained a characteristic comedo structure; (iii) the breast carcinoma was negative for estrogen receptor, progesterone receptor, and Her2 but positive for cytokeratin, which was negative in the FDC sarcoma; (iv) at the initial and second episodes of right axillary lymph node swelling, no tumor was found at any body site, despite extensive examination; (v) the breast carcinoma was negative for CD21, CD23, and CD35 as well as DAKO-FDC; (vi) no metastases were identified in the lymph nodes dissected in the mastectomy operation; and (vii) because epithelial markers are occasionally positive for the FDC sarcoma [15] they are not always evidence of metastatic carcinoma.

The chromosomal subband 21q11.2 involved in the translocation identified in this case was thought to be in a gene-poor region, which is known to encode only *HSPA13* (previously *STCH*) [16], NRIP1 (alias *RIP140*) [17], *TPTE* [18], *CNN2* [19], *USP25* [19], and *ABCC13* [20]. Although ABCC is reported to be strongly associated with human hematopoietic system, it is difficult to show whether the ABCC gene locus is truly involved in our case.

Finally, characterization of FDCs is very difficult because it is not currently possible to obtain FDC-rich specimens by purification. However, in the case of hematopoietic neoplasms, discovery and characterization

of certain cytogenetic abnormalities have identified genes highly associated with specific subtypes (e.g., the cyclin D1 gene *CCND1* in mantle cell lymphoma and the *MALT1* gene in marginal zone B-cell lymphoma). Future detailed analysis of the 21q11.2 region, which is involved in the FDC sarcoma in our case, may yield new insights into the biology of FDC sarcoma.

References

[1] Pileri SA, Grogan TM, Harris NL, Banks P, Campo E, Chan JK, Favera RD, Delsol G, De Wolf-Peeters C, Falini B, Gascoyne RD, Gaulard P, Gatter KC, Isaacson PG, Jaffe ES, Kluin P, Knowles DM, Mason DY, Mori S, Müller-Hermelink HK, Piris MA, Ralfkiaer E, Stein H, Su IJ, Warnke RA, Weiss LM. Tumours of histiocytes and accessory dendritic cells: an immunohistochemical approach to classification from the International Lymphoma Study Group based on 61 cases. Histopathology 2002;41:1–29.

[2] Bofill M, Akbar AN, Amlot PL. Follicular dendritic cells share a membrane-bound protein with fibroblasts. J Pathol 2000;191:217–26.

[3] Soriano AO, Thompson MA, Admirand JH, Fayad LE, Rodriguez AM, Romaguera JE, Hagemeister FB, Pro B. Follicular dendritic cell sarcoma: a report of 14 cases and a review of the literature. Am J Hematol 2007;82:725–8.

[4] Chan JK, Fletcher CD, Nayler SJ, Cooper K. Follicular dendritic cell sarcoma: clinicopathologic analysis of 17 cases suggesting a malignant potential higher than currently recognized. Cancer 1997;79:294–313.

[5] Nakashima T, Kuratomi Y, Shiratsuchi H, Yamamoto H, Yasumatsu R, Yamamoto T, Komiyama S. Follicular dendritic cell sarcoma of the neck: a case report and literature review. Auris Nasus Larynx 2002;29:401–3.

[6] Chen WC, Jones D, Ho CL, Cheng CN, Tseng JY, Tsai HP, Chang KC. Cytogenetic anomalies in hyaline vascular Castleman disease: report of two cases with reappraisal of histogenesis. Cancer Genet Cytogenet 2006;164:110–7.

[7] Pauwels P, Dal Cin P, Vlasveld LT, Aleva RM, van Erp WF, Jones D. A chromosomal abnormality in hyaline vascular Castleman's disease: evidence for clonal proliferation of dysplastic stromal cells. Am J Surg Pathol 2000;24:882–8.

[8] Yakushijin Y, Shikata H, Kito K, Ohshima K, Kojima K, Hato T, Hasegawa H, Yasukawa M. Follicular dendritic cell tumor as an unknown primary tumor. Jpn Soc Clin Oncol 2007;12:56–8.

[9] Jiang L, Admirand JH, Moran C, Ford RJ, Bueso-Ramos CE. Mediastinal follicular dendritic cell sarcoma involving bone marrow: a case report and review of the literature. Ann Diag Pathol 2006;10: 357–62.

[10] Muñoz-Fernández R, Blanco FJ, Frecha C, Martín F, Kimatrai M, Abadía-Molina AC, García-Pacheco JM, Olivares EG. Follicular dendritic cells are related to bone marrow stromal cell progenitors and to myofibroblasts. J Immunol 2006;177:280–9.

[11] Sander B, Middel P, Gunawan B, Schulten HJ, Baum F, Golas MM, Schulze F, Grabbe E, Parwaresch R, Fuzesi L. Follicular dendritic cell sarcoma of the spleen. Hum Pathol 2007;38:668–72.

[12] Riedel F, Back W, Götte K, Hörmann K. Follicular dendritic reticulum cell sarcoma in a cervical lymph node. HNO 2001;49:837–41. [In German].

[13] Jones D, Amin M, Ordonez NG, Glassman AB, Hayes KJ, Medeiros LJ. Reticulum cell sarcoma of lymph node with mixed dendritic and fibroblastic features. Mod Pathol 2001;14:1059–67.

[14] Varadarajan R, Edge SB, Yu J, Watroba N, Janarthanan BR. Prognosis of occult breast carcinoma presenting as isolated axillary nodal metastasis. Oncology 2006;71:456–9.

[15] Fonseca R, Yamakawa M, Nakamura S, van Heerde P, Miettinen M, Shek TW, Myhre Jensen O, Rousselet MC, Tefferi A. Follicular dendritic cell sarcoma and interdigitating reticulum cell sarcoma: a review. Am J Hematol 1998;59:161–7.

[16] Reeves RH, Rue E, Yu J, Kao FT. *Stch* maps to mouse chromosome 16, extending the conserved synteny with human chromosome 21. Genomics 1998;49:156–7.

[17] Katsanis N, Ives JH, Groet J, Nizetic D, Fisher EM. Localisation of receptor interacting protein 140 (*RIP140*) within 100 kb of *D21S13* on 21q11, a gene-poor region of the human genome. Hum Genet 1998;102:221–3.

[18] Tapparel C, Reymond A, Girardet C, Guillou L, Lyle R, Lamon C, Hutter P, Antonarakis SE. The *TPTE* gene family: cellular expression, subcellular localization and alternative splicing. Gene 2003;323: 189–99.

[19] Valero R, Marfany G, González-Angulo O, González-González G, Puelles L, Gonzàlez-DuarteUSP25 R. a novel gene encoding deubiquitinating enzyme, is located in the gene-poor region 21q11.2. Genomics 1999;62:395–405.

[20] Yabuuchi H, Takayanagi S, Yoshinaga K, Taniguchi N, Aburatani H, Ishikawa T. ABCC13, an unusual truncated ABC transporter, is highly expressed in fetal human liver. Biochem Biophys Res Commun 2002;299:410–7.

Japanese phase II study of ^{90}Y-ibritumomab tiuxetan in patients with relapsed or refractory indolent B-cell lymphoma

Kensei Tobinai,[1,19] Takashi Watanabe,[1] Michinori Ogura,[3,20] Yasuo Morishima,[3] Tomomitsu Hotta,[4,21] Kenichi Ishizawa,[5] Kuniaki Itoh,[6] Shin-ichiro Okamoto,[8] Masafumi Taniwaki,[9] Norifumi Tsukamoto,[10] Hirokazu Okumura,[12] Takashi Terauchi,[13] Shigeru Nawano,[7,22] Masaki Matsusako,[14] Yoshihiro Matsuno,[2,23] Shigeo Nakamura,[15] Shigeo Mori,[16] Yasuo Ohashi,[17] Masaki Hayashi[18,24] and Keigo Endo[11]

[1]Hematology and Stem Cell Transplantation Division, [2]Clinical Laboratory Division, National Cancer Center Hospital, 5-1-1 Tsukiji, Chuo-ku, Tokyo, 104-0045; [3]Department of Hematology and Cell Therapy, Aichi Cancer Center Hospital, 1-1 Kanokoden, Chikusa-ku, Nagoya, 464-8681; [4]Department of Hematology and Oncology, Tokai University School of Medicine, 143 Shimokasuya, Isehara, Kanagawa, 259-1193; [5]Department of Rheumatology and Hematology, Tohoku University Hospital, 1-1 Seirho-cho, Aoba-ku, Sendai, 980-8574; [6]Division of Oncology/Hematology, [7]Diagnostic Radiology Division, National Cancer Center Hospital East, 6-5-1, Kashiwanoha, Kashiwa, Chiba, 277-8577; [8]Division of Hematology/Infectious Disease/Rheumatology, School of Medicine, Keio University, 35 Shinano-machi, Shinjuku-ku, Tokyo, 160-8582; [9]Department of Hematology and Oncology, Kyoto Prefectural University of Medicine, 465 Kajii-machi, Hirokoji Noboru, Kawara-machi-dori, Kamikyo-ku, Kyoto, 602-8566; [10]Department of Medicine and Clinical Science, [11]Department of Diagnostic Radiology and Nuclear Medicine, Gunma University Graduate School of Medicine, 3-39-15 Showa-machi, Maebashi, 371-8511; [12]Department of Cellular Transplantation Biology, Kanazawa University Graduate School of Medical Science, 13-1 Takara-cho, Kanazawa, 920-8641; [13]Cancer Screening Division, Research Center for Cancer Prevention and Screening, National Cancer Center, 5-1-1 Tsukiji, Chuo-ku, Tokyo, 104-0045; [14]Department of Radiology, St Lukes International Hospital, 9-1 Akashi-cho, Chuo-ku, Tokyo 104-8560; [15]Department of Pathology, Nagoya University Hospital, 65 Tsurumai-Cho, Showa-ku, Nagoya, 466-8560; [16]Department of Pathology, Teikyo University School of Medicine, 2-11-1 Kaga, Itabashi-ku, Tokyo, 173-8606; [17]Department of Biostatistics, School of Public Health, University of Tokyo, 7-3-1 Hongo, Bunkyo-ku, Tokyo, 113-8655; [18]Department of Clinical Development, Bayer HealthCare, 3-5-36 Miyahara, Yodogawa-ku, Osaka, 532-8577, Japan

(Received August 5, 2008/Accepted September 6, 2008/Online publication October 29, 2008)

There is no data about the efficacy and safety of radioimmunotherapy with ^{90}Y-ibritumomab tiuxetan in patients with relapsed or refractory indolent B-cell lymphoma pretreated with rituximab-containing chemotherapy. We focused on this in a Japanese phase II study. Radioimmunotherapy with ^{90}Y-ibritumomab tiuxetan (11.1 and 14.8 MBq) was evaluated in patients with 100–149 $\times$ 10^9 and >150 $\times$ 10^9 platelets/L, respectively. The primary endpoint was the overall response rate. Forty patients were treated with ^{90}Y-ibritumomab tiuxetan (18 with 11.1 MBq/kg and 22 with 14.8 MBq/kg). Thirty-five patients (88%) had been pretreated with rituximab, including 27 (68%) pretreated with rituximab-containing chemotherapy. The overall response rate was 83% (33/40; 95% confidence interval, 67–93%), and the complete response rate was 68% (27/40; 95% confidence interval, 51–81%). The overall response rates in patients pretreated with rituximab-containing chemotherapy and rituximab plus cyclophosphamide, doxorubicin, vincristine, and prednisone (R-CHOP) were 83% (19/23) and 94% (17/18), respectively. The median progression-free survival time of the 40 patients who received ^{90}Y-ibritumomab tiuxetan was 9.6 months. Toxicity was primarily hematological and mostly transient. No grade 4 non-hematological toxicity was observed. In conclusion, radioimmunotherapy with ^{90}Y-ibritumomab tiuxetan is safe and highly effective in patients with relapsed or refractory indolent B-cell lymphoma, including those pretreated with rituximab-containing chemotherapy. (ClinicalTrials.gov number NCT00220285) (*Cancer Sci* 2009; 100: 158–164)

Indolent B-cell non-Hodgkin lymphoma (B-NHL) usually presents with disseminated disease, and most patients are incurable with conventional treatments. When the disease is found early (stage I or II), a considerable fraction of patients can be cured by radiation therapy.[1,2] Rituximab, a chimeric anti-CD20 monoclonal antibody, has been shown to be effective in the treatment of relapsed or refractory indolent B-NHL,[3,4] and has been incorporated into the first-line treatment of indolent B-NHL, in combination with chemotherapy, including cyclophosphamide, doxorubicin, vincristine, and prednisone (CHOP), cyclophosphamide, vincristine, and prednisone, and fludarabine.[5–9]

Monoclonal antibodies conjugated with radionucleotides have been developed to deliver radiation to targeted sites of disease. Yttrium-90 (^{90}Y) ibritumomab tiuxetan (Y2B8) radioimmunotherapy (RIT) was approved by the US Food and Drug Administration for the treatment of relapsed or refractory low-grade, follicular or transformed B-NHL. Witzig *et al.* demonstrated that rituximab-refractory patients with low-grade B-NHL could be safely and effectively treated with Y2B8.[10] The absorbed radiation dose assessments indicated that normal organ dose in the study was consistent with doses observed in other trials for patients previously untreated with rituximab.[11] Previously, we reported the results of a Japanese phase I study, showing that the recommended dose of Y2B8 for the subsequent phase II study with 150 $\times$ 10^9 or more platelets/L is 14.8 MBq/kg (0.4 mCi/kg), and that RIT with Y2B8 appeared to be highly effective and well tolerated in Japanese patients mostly pretreated with rituximab, with similar pharmacokinetic and safety profiles to Western populations.[12] However, no data on Y2B8 RIT for patients with indolent B-NHL previously treated with rituximab-containing chemotherapy (R-chemo) have been published. Thus, we conducted a multicenter phase II study to evaluate the efficacy and safety of Y2B8 RIT for Japanese patients with relapsed or refractory indolent B-NHL, focusing on those pretreated with R-chemo.

Patients and Methods

This was a multicenter phase II study to evaluate the safety and efficacy of ^{111}In- and ^{90}Y-ibritumomab tiuxetan in relapsed or refractory patients with indolent B-NHL. The primary endpoint

[19]To whom correspondence should be addressed. E-mail: ktobinai@ncc.go.jp
The Present addresses of the authors different from those where the work was carried out are as follows: [20]Department of Hematology and Oncology, Nagoya Daini Red Cross Hospital, 2-9 Myoken-cho, Showa-ku, Nagoya, 466-8650; [21]Nagoya Medical Center, 4-1-1 San-nomaru, Naka-ku, Nagoya, 460-0001; [22]Department of Radiology, IUHW Mita Hospital, 1-4-3 Mita, Minato-ku, Tokyo, 108-8329; [23]Department of Pathology, Hokkaido University Hospital, Kita 14, Nishi 5, Kita-ku, Sapporo, 060-8648; [24]Department of Internal Medicine, Nakagami Hospital, 6-25-5 Chihana, Okinawa, 904-2195, Japan.

doi: 10.1111/j.1349-7006.2008.00999.x

was the overall response rate (ORR), and the primary safety variable was the incidence of critical toxicities defined as follows: (1) grade 4 thrombocytopenia or platelet transfusions according to the National Cancer Institute-Common Toxicity Criteria version 2.0; (2) life-threatening hemorrhage; and (3) death caused by toxicity. Complete response rate (%CR) and progression-free survival (PFS) were the secondary endpoints. The study was approved by the institutional review boards of the participating institutions, and written informed consent was obtained from all patients.

Patient eligibility. The protocol required relapsed or refractory patients to have histologically confirmed indolent B-NHL according to the International Working Formulation[13] and World Health Organization classification[14] (small lymphocytic, lymphoplasmacytic, mantle cell, follicular center [grades I, II, and III], marginal zone B-cell, and splenic marginal zone lymphoma). Patients who showed histological transformation to aggressive B-NHL were eligible. Those patients who met the following criteria were enrolled: bidimensionally measurable disease with the longest diameter of 2.0 cm or longer by computed tomography or magnetic resonance imaging; a demonstrable monoclonal CD20-positive B-cell population in lymphomatous lesions by flow cytometry or immunohistochemistry; neither prior therapy with rituximab for 3 months nor antineoplastic therapy 4 weeks prior to enrollment; and a performance status of 0 or 1 according to the Eastern Cooperative Oncology Group scale.[15] In addition, patients had to be 20–74 years old, not pregnant or lactating, using accepted birth control methods, and have a life expectancy of ≥3 months. Within 1 week prior to enrollment, patients were required to have acceptable hematological status (neutrophils $\geq 1.2 \times 10^9$/L and platelets $\geq 150 \times 10^9$/L), hepatic function (aspartate aminotransferase, alanine aminotransferase, and alkaline phosphatase ≤ 2.5 times normal, total bilirubin ≤ 2.0 mg/dL), and renal function (serum creatinine ≤ 2.0 mg/dL). Patients were excluded if they had the following conditions: prior stem cell transplantation; external beam radiation to bilateral ilium or whole abdomen; central nervous system lymphoma; chronic lymphocytic leukemia; human immunodeficiency virus-related lymphoma, lymphoma cells $> 5 \times 10^9$/L in peripheral blood; ≥25% bone marrow involvement with lymphoma cells; and lymphoma cells within pleural effusion or ascites.

Central pathology review. Unstained microscopic slides of lymphoma tissues obtained on initial biopsy or relapse were collected and stained with hematoxylin–eosin, and immunohistochemical analyses were conducted as described previously.[16] Preparations were examined microscopically by three hematopathologists (Yo.M., S.Nak., and S.M.). The diagnosis by the central review committee was regarded as the final diagnosis.

Treatment. The treatment consisted of the following components as described previously:[12] rituximab (provided by Zenyaku Kogyo, Tokyo, Japan), ^{111}In-ibritumomab tiuxetan (In2B8), and ^{90}Y-ibritumomab tiuxetan (Y2B8). On day 1, patients received 129.5 MBq (3.5 mCi) In2B8 after pretreatment with 250 mg/m^2 rituximab. Three planar imaging scans were acquired by γ camera at 2–24, 48–72, and 90–144 h after administration of In2B8. On 1 day from day 7–9 after the In2B8 injection, patients received a single intravenous injection of Y2B8 after pretreatment with rituximab (250 mg/m^2). Y2B8 was injected only after the γ images confirmed the absence of an altered biodistribution, according to the recommendation by Conti and coworkers on the image interpretation criteria.[17] The dose of Y2B8 was 14.8 MBq/kg (0.4 mCi/kg) for patients with platelets of $\geq 150 \times 10^9$/L, and 11.1 MBq/kg (0.3 mCi/kg) for patients with platelets of $\geq 100 \times 10^9$/L to $< 150 \times 10^9$/L, based on the results of the preceding US study for patients with mild thrombocytopenia.[18] The maximum dose of Y2B8 was limited to 1184 MBq/kg (32 mCi/kg).

Response evaluation. Response was assessed at 8 and 12 weeks after the Y2B8 injection, in accordance with the International Workshop Response Criteria for NHL.[19] In addition to the efficacy evaluation at each participating institute, an independent, third-party panel of three radiologists (T.T., S. Naw., and M.M.) carried out a central evaluation using the collected computed tomography films. Patients were followed up to 3 months after the last enrolled patient completed the protocol treatment, and if there was apparent progressive disease (PD), it was reported.

Evaluation of toxicity and safety. All adverse events (AE) were followed for up to 13 weeks after the first rituximab infusion, and were graded according to the National Cancer Institute-Common Toxicity Criteria version 2.0. All adverse drug reactions that persisted after 13 weeks and those occurring during the follow-up period were followed until resolution.

In total, 89 doses of ibritumomab tiuxetan were radiolabeled for treatment at study sites: 44 radiolabeled with ^{90}Y and 45 with ^{111}In. Of these, 4 of 44 doses with ^{90}Y did not exceed the release specification of 95% for the radioincorporation assay, whereas all 45 doses with ^{111}In exceeded the specification.

Statistical analysis. As most patients enrolled in the study were anticipated to have received R-chemo, the expected ORR was set at 60%, considering the lower limit of the 95% confidence interval (CI) (60–85%) for the ORR of 74% (40/54) from the US phase II trial for rituximab-refractory patients.[10] The threshold ORR was set at 35% because this therapy is expected to show a higher ORR than that by rituximab retreatment (38–40%).[20,21] With the level of significance at 5% (one tailed), the required sample size to attain a statistical power of 80% was 28 patients.

Regarding the primary safety variable of critical toxicity, its expected incidence was set at 15%, considering the incidence (13%; 4/30) of grade 4 thrombocytopenia ($< 10 \times 10^9$/L) in patients with baseline platelet counts of $\geq 100 \times 10^9$/L to $< 150 \times 10^9$/L who received Y2B8 of 11.1 MBq/kg (0.3 mCi/kg) in the preceding US study,[18] and the threshold incidence was set at 50%. With the level of significance at 5% (one tailed), the required sample size to attain a statistical power of 90% was calculated to be 16 patients. The analysis applied in each subgroup of patients with baseline platelets of $\geq 150 \times 10^9$/L and $\geq 100 \times 10^9$/L to $< 150 \times 10^9$/L, because there might have been a different response between the subgroups due to differences in bone marrow reserves. Therefore, the targeted enrollment was set at 40 patients: at least 16 with baseline platelet counts of $\geq 150 \times 10^9$/L and at least 16 with counts of between 100×10^9/L and 150×10^9/L.

Data were analyzed for all patients who received any study drug. Primary variables and toxicities were analyzed in the 40 patients who received Y2B8. PFS, which was defined as the period of time from the date of enrollment to that of the assessment of PD, the date of death due to any cause, or the date necessitating other antilymphoma treatment (whichever occurred earlier) was analyzed with the use of the Kaplan–Meier method.

Results

Patients. From July 2004 to October 2005, 47 patients were enrolled, and 45 of them received In2B8. Two patients did not receive the study medications at all because of early PD immediately after enrollment in one patient and human antimurine antibody positivity in the other. Of 45 patients who received In2B8, five did not receive Y2B8 because of a baseline neutrophil count of less than 1.2×10^9/L in one patient and suspected altered distribution in the remaining four. Based on a central review of the imaging interpretation, two of the four patients were judged to have an altered biodistribution (prominent bone marrow), whereas the remaining two were within the range of the expected biodistribution. Of the 40 patients who received Y2B8, 18 received 11.1 MBq/kg (0.3 mCi/kg), and 22 received